Parallel Functional Interrogations of Autism Risk Genes Reveal Drivers of Transcriptomic Convergence and the Female Protective Effect

Rebecca E. Andersen[1,2,3,4,*], Maya Talukdar[1,2,3,5,*], Tyler Sakamoto[1,6], David Exposito-Alonso[1,2,4,7,8], Janet H.T. Song[1,2,4,7,8], Xuyu Qian[1,2,4,7,8], Seungil Lee[1,6], Nila Murugan[1,9], Ryan N. Delgado[10], Sijing Zhao[1,11], Gwenyth Eichfeld[1,12], Julia Harms[1,13], David C. Page[14,15,16], and Christopher A. Walsh[1,2,3,4,7,8]

Affiliations:
[1]Division of Genetics and Genomics and Manton Center for Orphan Diseases, Boston Children's Hospital, Boston, MA, USA; [2]Department of Pediatrics, Harvard Medical School, Boston, MA, USA; [3]Broad Institute of MIT and Harvard, Cambridge, MA, USA; [4]Allen Discovery Center for Human Brain Evolution, Boston, MA, USA; [5]Harvard-MIT MD/PhD Program, Program in Biomedical Informatics, Boston, MA, USA; [6]Harvard College, Cambridge, MA, USA; [7]Howard Hughes Medical Institute, Boston Children's Hospital, Boston, MA, USA; [8]Department of Neurology, Harvard Medical School, Boston, MA, USA; [9]University of Massachusetts Boston, Boston, MA, USA; [10]Department of Genetics, Blavatnik Institute, Howard Hughes Medical Institute, Harvard Medical School, Boston, MA, USA; [11]Harvard BBS PhD Program, Boston, MA, USA; [12]Colgate University, Hamilton, NY, USA; [13]University of California Berkeley, Berkeley, CA, USA; [14]Whitehead Institute, Cambridge, MA 02142, USA; [15]Department of Biology, Massachusetts Institute of Technology, Cambridge, MA 02139, USA; [16]Howard Hughes Medical Institute, Whitehead Institute, Cambridge, MA 02142, USA.

*These authors contributed equally.

Corresponding author and lead contact:

Christopher A. Walsh, christopher.walsh@childrens.harvard.edu

SUMMARY

The surprising number and functional diversity of genes implicated in autism spectrum disorder (ASD) has made it challenging to identify core pathophysiological mechanisms or envision interventions with broad therapeutic potential. Here, parallel CRISPR-Cas13-based knockdown of 28 ASD genes and neighboring long non-coding RNAs reveals striking convergence on shared transcriptomic effects and neurodevelopmental phenotypes in human neural progenitor cells and cerebral organoids. Perturbations of single ASD genes caused the widespread dysregulation of other ASD genes, and *de novo* reconstruction of gene regulatory networks uncovered the prominent autism risk gene *CHD8* as a critical driver of this transcriptomic convergence. The transcriptional activator *ZFX*, which escapes X chromosome inactivation in females, was also identified as a key regulator of ASD genes, revealing genetic underpinnings of the female protective effect. Thus, this study provides a crucial framework for uncovering how variants in diverse genes can cause convergent pathophysiological effects that ultimately result in a shared diagnosis.

INTRODUCTION

Autism spectrum disorder (ASD) is a common neurodevelopmental condition characterized by deficits in social communication as well as restricted and/or repetitive behaviors. Although ASD is clinically heterogeneous, these central features can be used diagnostically to distinguish ASD from other neurodevelopmental disorders (DSM-5, 2013), indicating that certain biological foundations of ASD are shared across individuals. Moreover, ASD has a significant genetic component (Bai et al. 2019), and several large-scale studies have identified genes implicated in ASD (ASD genes) (Grove et al. 2019; Satterstrom et al. 2020; Trost et al. 2022). These studies have enabled the compilation of ASD genes into large databases such as the Simons Foundation Autism Research Initiative (SFARI) Gene database (Abrahams et al. 2013), which has surprisingly revealed that hundreds of genes with diverse functions are implicated in ASD. Understanding how disruptions in such seemingly disparate genes lead to the core pathophysiology of ASD remains a major challenge (Liao et al. 2023).

Furthermore, while previous studies have primarily focused on identifying protein-coding genes (PCGs) implicated in ASD, there is emerging evidence that non-coding sequences can also play important roles in brain development. For instance, genetic disruptions in multiple long non-coding RNAs (lncRNAs) have now been implicated in ASD (Noor et al. 2010; Luo et al. 2018; Ang et al. 2019; Andersen et al. 2024), suggesting that mutations in lncRNAs can cause ASD. Moreover, transcriptomic analyses of ASD brain tissue have found that lncRNAs are frequently dysregulated in ASD (Ziats and Rennert 2013; Parikshak et al. 2016), including lncRNAs that are in close proximity to ASD-associated PCGs. As certain classes of lncRNAs have been found to modulate the expression and/or function of their nearby genes (Luo et al. 2016; Wang et al. 2020), this raises the possibility that lncRNAs neighboring ASD PCGs could play particularly critical roles in ASD-relevant molecular pathways even if they are not directly disrupted.

Additionally, ASD has a significantly higher prevalence in males, with approximately 3-4 males diagnosed for every female (Loomes et al. 2017; Maenner et al. 2023). Although ASD genes have

been identified on the X chromosome (Mendes et al. 2024), X-linked causes of ASD alone cannot fully explain the male-biased prevalence of ASD (Ropers and Hamel 2005; Werling 2016; Martin et al. 2021). Moreover, females with ASD tend to have a greater genetic load of autosomal ASD variants than males (Jacquemont et al. 2014; Pinto et al. 2014; Zhang et al. 2020; Napolitano et al. 2022; Wigdor et al. 2022; Antaki et al. 2022; Warrier et al. 2022), suggesting that females require more autosomal genetic risk to manifest ASD. However, the genetic mechanisms of this "female protective effect" (Werling 2016; Dougherty et al. 2022) have yet to be uncovered.

Here, functional interrogation of ASD genes and neighboring lncRNAs in human neural progenitor cells (NPCs) and cerebral organoids reveals remarkably widespread transcriptomic convergence, which we define as statistically significant overlap of the same individual differentially expressed genes (DEGs) across different conditions. Strikingly, most perturbations resulted in DEGs that were enriched for other ASD genes. *De novo* reconstruction of a gene regulatory network (GRN) enabled the identification of central regulators, including the well-known ASD gene *CHD8* as well as novel candidates such as *REST*, that drive transcriptomic convergence in ASD. Furthermore, the X-linked transcriptional activator *ZFX*, which escapes X chromosome inactivation (XCI) in females, emerged as a key regulator of ASD genes, demonstrating that expression from the "inactive" X chromosome is an important biological foundation of the female protective effect. Disruption of several ASD genes and neighboring lncRNAs also led to phenotypic convergence, affecting the critical processes of proliferation in NPC cultures and neurogenesis in cerebral organoids. Thus, this work reveals how key GRNs become broadly dysregulated upon disruption of a single ASD gene, uncovering molecular mechanisms of transcriptomic convergence in ASD. Moreover, these results highlight central regulators such as *CHD8* and *REST*, which are promising targets for future therapeutic interventions that could provide broad benefits across diverse genetic causes of ASD.

RESULTS

Consensus-ASD Reveals Shared and Unique Features Across Classes of Genetic Variation

The genetic underpinnings of ASD have primarily been investigated in the context of genes that are recurrently disrupted by rare *de novo* copy number variants (CNVs) or single nucleotide variants (SNVs) in ASD. However, ASD has a complex genetic architecture with contributions from multiple distinct genetic variant classes (Iakoucheva et al. 2019; Dias and Walsh 2020; Willsey et al. 2022). Thus, we first systematically aggregated variants implicated in ASD from 32 different studies across seven different genetic variant classes: 1) germline SNVs and indels implicated in idiopathic ASD, 2) syndromic variants with ASD as a recurrent feature, 3) somatic SNVs and indels, 4) germline CNVs, 5) somatic CNVs, 6) inherited recessive variants, and 7) common variants (GWAS SNPs). This dataset, which we refer to as *Consensus-ASD* (**Fig. 1A**), enabled us to identify shared and unique features across variant classes (**Fig. S1-S2** and **Table S1**), highlighting differences in genetic constraint (Lek et al. 2016) and developmental expression patterns.

Depletion of ASD Genes and Adjacent lncRNAs Causes Similar Effects on Gene Expression

Functional interrogation of ASD genes and their adjacent lncRNAs revealed strongly overlapping effects on downstream targets. Knockdown (KD) studies were performed for a total of 38 genes, including 19 SFARI genes and 17 neighboring lncRNAs, as closely adjacent lncRNAs have often been found to regulate the expression and/or function of their neighbors (Villegas and Zaphiropoulos 2015; Luo et al. 2016; Wang et al. 2020). This included the lncRNA *NR2F1-AS1*, which has itself been implicated in ASD (Ang et al. 2019). *NR2F1-AS1* is adjacent to the SFARI gene *NR2F1*, which was also included in our study. Additionally, we included the lncRNA *SOX2-OT*, a lncRNA recently implicated in ASD (Andersen et al. 2024), along with its overlapped protein-coding gene (PCG) *SOX2*, a transcription factor known to play important roles in neural development (Graham et al. 2003; Lee et al. 2014).

120 For each of these genes (**Table S2**), CRISPR-Cas13 (Konermann et al. 2018; Wei et al.
121 2023) and an array of three guide RNAs (gRNAs) targeting the gene (**Table S3**) were used for
122 KD in human XY (male) NPC cultures (**Fig. 1B-C**). RNA-seq was performed after 24 hours to
123 determine the acute effects of these perturbations. Most (28/38, 73.7%) of the target genes
124 exhibited statistically significant KD relative to non-targeting control (NTC) samples (**Fig. 1D** and
125 **Table S4**), including 19/20 (95%) of the PCGs and 9/18 (50%) of the lncRNAs. Subsequent
126 analyses were limited to the 28 conditions that demonstrated significant KD.
127 While only 1 lncRNA (1/19, 5.26%) was significantly differentially expressed upon KD of its
128 neighboring PCG, the majority of lncRNA KDs (5/9, 55.6%) led to significant differential
129 expression of their neighboring PCG (**Fig. 1E** and **S3**). Of these, most (4/5, 80%) of the lncRNA
130 KDs resulted in decreased expression of the PCG neighbor, consistent with previous reports
131 that closely adjacent lncRNAs often positively regulate the expression of their nearby neighbors
132 (Villegas and Zaphiropoulos 2015; Luo et al. 2016; Wang et al. 2020). Transcriptome-wide
133 analysis, limited to the 25 samples with at least 50 differentially expressed genes (DEGs),
134 revealed a strong and significant correlation in fold change of DEGs between each neighboring
135 lncRNA-PCG pair (8/8, $p < 2.2e-16$ in each comparison; testing beta $\neq 0$) (**Fig. S4**). Linear
136 modeling determined that lncRNA-KD fold changes were smaller than PCG-KD fold changes on
137 a per-gene basis (8/8, $p < 2.2e-16$ in each comparison; testing beta < 0) (**Fig. S4**), indicating
138 that perturbation of these lncRNAs and their neighboring PCGs affect shared downstream
139 genes but that the magnitude of the effect tends to be weaker upon KD of the lncRNA. This is
140 consistent with lncRNAs often functioning to fine-tune the expression of critical genes and
141 signaling pathways (Zhao et al. 2021). Thus, lncRNAs adjacent to ASD genes, and particularly
142 the lncRNAs highlighted here, warrant further consideration as potential contributors to ASD.
143
144 <u>ASD-Related Perturbations Result in Widespread Dysregulation of Other ASD Genes</u>

145 Transcriptome-wide analysis revealed that the ASD-relevant perturbations caused
146 remarkably broad disruption of other ASD genes. Most sets of DEGs from the individual KDs
147 exhibited enrichment for genes in *Consensus-ASD* (21/25, 84%) (**Fig. 2A**) as well as SFARI
148 genes (19/25, 76%) (**Fig. S5A**). This enrichment was uniformly weaker when considering genes
149 implicated in intellectual disability (SysID) (Kochinke et al. 2016) (**Fig. S5A**), suggesting that
150 perturbation of ASD genes particularly affects other ASD genes as opposed to
151 neurodevelopmental genes more broadly. Thus, perturbation of known ASD genes and
152 neighboring lncRNAs leads to widespread disruption of other ASD genes.
153 Surprisingly, we found a striking pattern of transcriptomic convergence on the same individual
154 DEGs across the different perturbations. This was particularly evident when focusing on high
155 confidence SFARI (HC-SFARI) genes, the SFARI genes in the highest evidentiary tier for
156 association with ASD (**Fig. 2B**). Not only were the same specific genes shared across multiple
157 perturbations, but they were also largely affected in the same direction by the different KDs.
158 Moreover, HC-SFARI genes tended to shift in a concordant direction as a result of the different
159 perturbations even when they did not rise to the level of a statistically significant DEG within a
160 particular KD sample (**Fig. 2C** and **S5B**). While previous functional studies of ASD genes have
161 identified certain overlapping changes in cell type composition and behavior, evidence of
162 transcriptomic convergence is quite limited (Paulsen et al. 2022; Weinschutz Mendes et al. 2023;
163 Li et al. 2023). Indeed, based on functional studies in cerebral organoids it has been proposed
164 that different ASD mutations largely impact distinct downstream genes (Paulsen et al. 2022).
165 Thus, the strong convergence on shared ASD DEGs that we observed across numerous ASD
166 perturbations was highly unexpected. Nevertheless, common patterns of DEGs have been
167 identified in brain tissue from ASD cases compared to neurotypical controls (Voineagu et al. 2011;
168 Parikshak et al. 2016; Ramaswami et al. 2020; Gandal et al. 2022), consistent with our findings.
169 Further analysis of transcriptomic convergence enabled the discovery of candidate ASD risk
170 genes. We identified genes with following features: 1) significantly downregulated by at least three

171 of the ASD KDs; 2) at least 80% concordant in the direction of significant differential expression
172 across all ASD KDs; and 3) intolerant to loss of function variants, as determined by LOEUF scores
173 of less than 0.6 ("constrained"). This analysis resulted in a set of 584 genes (**Table S5**), of which
174 138 (23.6%) were SFARI genes. This strong enrichment (p = 6.47e-08) of SFARI genes within
175 the candidate ASD risk genes demonstrates that these criteria can effectively prioritize genes that
176 indeed contribute to ASD.
177
178 Key Transcription Factors Including *REST* Target Recurrently Differentially Expressed Genes
179 Transcription factors (TFs) that mediate transcriptomic convergence in ASD were uncovered
180 through MAGIC analysis (Roopra 2020), which identified TFs whose target genes were
181 significantly differentially expressed in at least 20/25 (80%) of the perturbations (recurrent
182 MAGIC TFs) (**Fig. 2D** and **S5C**). Many of these significant TFs are involved in pathways or
183 complexes previously linked to ASD, such as SWI/SNF (Wenderski et al. 2020; Valencia et al.
184 2023), WNT (Kalkman 2012), and CTCF (Price et al. 2023), or have themselves been
185 implicated in ASD. Of the recurrent MAGIC TFs that have not been directly implicated in ASD,
186 several exhibited high genetic constraint and co-expression with known ASD genes, features
187 that have been used to nominate candidate ASD risk genes (Liao et al. 2023).
188 Of particular interest, RE1 silencing transcription factor (REST) was a significant MAGIC TF
189 in 24/25 (96%) of our perturbations. While REST has not previously been directly associated
190 with ASD, it is known to carry out critical neurodevelopmental roles, functioning as a master
191 negative regulator of neurogenesis (Schoenherr and Anderson 1995; Chong et al. 1995). Re-
192 analysis of REST binding sites from embryonic stem cells (ESCs) (Rockowitz and Zheng 2015)
193 revealed strong enrichment of SFARI and *Consensus-ASD* genes within REST target genes
194 from both human (adj. p = 2.7e-47 and 1.0e-43, respectively) and mouse (adj. p = 4.2e-40 and
195 4.2e-40, respectively) (**Fig. 2E**). Genes implicated in intellectual disability (SysID) were also
196 enriched (adj. p = 7.6e-13 and 2.3e-10, respectively); however, this enrichment was notably

197 weaker than that for ASD genes, suggesting that REST is especially important in regulating
198 ASD-relevant gene expression.
199
200 Gene Regulatory Network Analysis Identifies *CHD8* as a Top Driver of Convergence in ASD
201 *De novo* reconstruction of an NPC gene regulatory network (GRN) uncovered critical
202 regulatory relationships underlying transcriptomic convergence. The bioinformatic tool ARACNe
203 (Margolin et al. 2006; Lachmann et al. 2016) was used to build GRNs linking transcription
204 factors (Lambert et al. 2018) and epigenetic regulators (Boukas et al. 2019) to their downstream
205 targets (regulons). To confirm the validity of this approach, we first constructed a GRN that
206 excluded data from the seven samples in which the KD target was a potential regulator, which
207 enabled evaluation of the predictive ability of the ARACNe-derived GRN through comparison
208 with the held-out RNA-seq data. For all 7/7 (100%) of the KDs, strong and significant cross-
209 enrichment was found between the downregulated DEGs and the 1st and 2nd degree ARACNe
210 regulons (i.e., direct targets as well as their direct targets) ($p < 2.2e-16$, Fisher's combined
211 probability test) (**Fig. 3A** and **S6**). Thus, ARACNe is able to effectively capture true regulatory
212 relationships. We then built an ARACNe GRN from our full set of RNA-seq data. In total, this
213 identified 101,918 putative regulatory relationships between 1,098 known transcription factors or
214 epigenetic regulators and 9,464 target genes, including many highly interconnected
215 relationships between known ASD genes (**Fig. 3B**).
216 Genes implicated in ASD are central regulators of the NPC GRN, as demonstrated by
217 analysis using the PageRank algorithm (Page et al. 1999) (**Fig. 3C**). Genes in *Consensus-ASD*
218 were strongly enriched for high PageRank scores (adj. $p = 1.3e-9$), indicating their centrality to
219 the GRN. This enrichment was also significant for SFARI genes (adj. $p = 6.7e-4$), while SysID
220 genes demonstrated much weaker enrichment (adj. $p = 0.03$). Analysis of Hallmark Molecular
221 Signature Databases pathways (Subramanian et al. 2005) further identified strong enrichment
222 for genes associated with cell division and proliferation such as G2M checkpoint (adj. p = 1.8e-

223 3) and mitotic spindle (adj. p = 1.1e-4) within the top PageRank genes, consistent with previous
224 findings of ASD-related effects on NPC proliferation (Connacher et al. 2022) and tubulin biology
225 (Lasser et al. 2023; Sun et al. 2024; Kostyanovskaya et al. 2025).

226 Further GRN analysis identified key regulators driving transcriptomic convergence in ASD.
227 Regulators whose activity was consistently altered by the KD of ASD genes were identified
228 using the bioinformatic tool VIPER (Alvarez et al. 2016). Of these, we focused on top drivers of
229 convergence in ASD by identifying regulators whose targets were enriched for genes in
230 *Consensus-ASD* and for genes that are highly central to the network (i.e. gene with high
231 PageRank scores), which identified 78 key regulators (**Fig. S7**). Over half of these top
232 regulators are *Consensus-ASD* genes themselves (41/78, 52.6%, adj. p = 1.5e-19), and over
233 one quarter are HC-SFARI genes (21/78, 26.9%, adj. p = 2.e3-20). These top regulators
234 exhibited remarkably strong cross-regulation (p = 0), as determined by mean normalized degree
235 (**Fig. S7**). Analysis of the STRING database of protein-protein interactions (PPIs) (Szklarczyk et
236 al. 2023) further confirmed that these top regulators are highly interconnected (p = 2.75e-11,
237 STRING PPI Enrichment Score) (**Fig. S8**). Taken together, this suggests that these top
238 regulators not only modulate many ASD genes but also cross-regulate each other, driving
239 transcriptomic convergence in ASD.

240 Iterative walktrap clustering identified 5 gene modules within the 78 top regulators that were
241 especially strongly interconnected (**Fig. 3D** and **S9**). Of particular interest, the largest of these
242 (**Fig. S9C**) demonstrates a high degree of cross-interaction throughout the module and contains
243 several notable ASD genes including *CHD8*, one of the strongest known risk genes for ASD
244 (Haddad Derafshi et al. 2022). The inferred *CHD8* regulons from the GRN were strongly
245 enriched (1st degree regulon adj. p = 8.7e-8, 1st and 2nd degree regulon adj. p = 9.0e-24) for
246 genes that were previously identified as direct CHD8 targets through ChIP-seq from NPCs
247 (Sugathan et al. 2014) (**Fig. 3E**). The CHD8 ChIP-seq targets were also highly enriched for
248 genes in *Consensus-ASD* (adj. p = 4.64e-20), SFARI genes (adj. p = 1.13e-7), and HC-SFARI

249 genes (adj. p = 1.13e-7), further supporting the role of *CHD8* as a key regulator of ASD gene
250 expression.
251 Furthermore, the *CHD8*-containing module included three regulators (*SETD2*, *SETD5*, and
252 *KMT2E*) that we had directly perturbed and which we would predict to share many downstream
253 targets with *CHD8*. Indeed, the DEGs from these KDs also exhibited enrichment
254 for CHD8 ChIP-seq targets (adj. p = 8.81e-6, 1.60e-7, and 1.36e-4, respectively), further
255 demonstrating the convergent regulation of shared targets by critical ASD genes. Interestingly,
256 *CHD8* is not differentially expressed upon *KMT2E* KD; similarly, *KMT2E* was not identified as a
257 direct target of CHD8 by ChIP-seq (Sugathan et al. 2014). Consistent with this, ARACNe
258 analysis did not identify a direct interaction between *CHD8* and *KMT2E*. This suggests that even
259 ASD genes that do not directly regulate each other may jointly regulate a shared set of
260 downstream genes, leading to convergent changes upon their disruption. Moreover, this
261 analysis highlights *CHD8*, a high confidence ASD risk gene, as a key regulator driving
262 transcriptomic convergence in ASD.
263
264 <u>The X-Linked Transcription Factor *ZFX* is a Key Contributor to the Female Protective Effect</u>
265 Sex-differential patterns of gene expression could contribute to the female protective effect
266 (FPE) in ASD. Prior studies have found that autosomal genes that are disrupted or
267 downregulated in ASD tend to be more highly expressed in the brains of neurotypical females
268 compared to males, suggesting that female-biased expression of ASD-relevant genes may
269 contribute to the FPE (Werling et al. 2016; Velmeshev et al. 2023). We hypothesized that X-
270 linked transcriptional regulators that escape XCI could drive these female-biased expression
271 patterns. Thus, we first sought to identify constrained (LOEUF < 0.6) X-linked regulators of the
272 candidate ASD risk genes (**Table S5**) defined earlier in this study.
273 MAGIC analysis revealed 155 constrained regulators whose targets were significantly
274 enriched for candidate ASD risk genes (**Table S6**), including 39 regulators that are themselves

275 SFARI genes. Eight of the regulators were X-linked, and their targets were also found to be
276 significantly enriched within the full set of DEGs from many of the individual ASD gene KDs
277 (**Fig. 4A**). To further identify transcriptional regulators of candidate ASD risk genes, we
278 analyzed our NPC GRN, which identified 229 constrained regulators whose regulons were
279 significantly enriched for candidate ASD risk genes (**Table S7**), including 74 regulators that
280 were SFARI genes and ten regulators that were X-linked (**Fig. 4B** and **S10A**). Four of these X-
281 linked regulators could also be analyzed by MAGIC: all of them (4/4, 100%) were positively
282 identified as significant MAGIC regulators, further reinforcing the strongly concordant results
283 between these fundamentally different analytical approaches. Together, these analyses
284 identified 14 constrained X-linked regulators of candidate ASD risk genes, half of which (7/14,
285 50%) have themselves been implicated in ASD and are considered SFARI genes. This
286 highlights several X-linked genes that could contribute to the greater prevalence of ASD in
287 males through their regulation of candidate ASD risk genes (**Fig. 4C**).
288 We then sought to uncover regulators that could contribute to the FPE. Of the 14 regulators
289 identified above, only *ZFX* has been shown to escape XCI in females (San Roman et al. 2023)
290 and exhibit female-biased expression in the developing cerebral cortex (Kissel et al. 2024).
291 Indeed, *ZFX* is consistently found to be one of the most highly female-biased genes across a
292 variety of tissue and cell types (Oliva et al. 2020; Blanton et al. 2024). Moreover, *ZFX* is a
293 transcriptional activator that has been shown to mediate widespread upregulation of many
294 autosomal genes (Raznahan et al. 2018; San Roman et al. 2024), supporting its potential
295 contribution to the FPE. Interestingly, pathogenic variants in *ZFX* have recently been directly
296 implicated in ASD (Shepherdson et al. 2024). In our perturbation studies, KD of several different
297 ASD genes led to downregulation of *ZFX* (**Fig. 4D**), suggesting that decreased *ZFX* activity can
298 also occur in ASD without requiring direct mutations in *ZFX*. As females exhibit higher
299 expression of *ZFX*, they are better buffered against this change, and thus *ZFX* could contribute
300 to sex-differential outcomes even when it is not directly mutated.

301 We further investigated the role of *ZFX* in ASD through re-analysis of *ZFX* targets that were
302 previously identified based on ChIP-seq and CRISPR KD experiments in two separate cell lines
303 (San Roman et al. 2024). Our analysis demonstrated that these *ZFX* targets are enriched for
304 ASD-relevant gene sets including SFARI genes and genes that exhibit female-biased
305 expression in the brain (**Fig. 4E**). The enrichment of ASD-relevant gene sets was further
306 validated through re-analysis of additional ChIP-seq data (Rhie et al. 2018) (**Fig. S10B**).
307 Furthermore, we analyzed our NPC GRN and found that the *ZFX* 1st and 2nd degree regulon
308 includes many (12/78, 15.4%) of the top drivers of transcriptomic convergence in ASD that we
309 had previously identified (**Fig. 4F**). Thus, *ZFX* is an XCI-escaping female-biased regulator of
310 ASD risk genes that may provide a crucial foundation for the FPE by driving sex-differential
311 expression of genes that are disrupted in ASD.
312
313 <u>ASD Genes and Adjacent lncRNAs Regulate NPC Proliferation</u>
314 We next focused on uncovering potential phenotypic convergence and found that several
315 ASD gene perturbations caused similar effects on NPC proliferation. Analysis using the
316 heritable CytoTrack dye (**Fig. 5A**) revealed that 8/16 (50%) of the SFARI gene KDs led to a
317 statistically significant decrease in proliferation (**Fig. 5B** and **Table S8**). This was also the case
318 for the lncRNA *SOX2-OT*, which has previously been implicated in ASD (Andersen et al. 2024),
319 as well as its overlapped PCG *SOX2*, a TF known to regulate NPC proliferation (Graham et al.
320 2003; Lee et al. 2014). In contrast, 1/16 (6.25%) SFARI KDs and 3/8 (37.5%) lncRNA KDs led
321 to increased NPC proliferation (**Fig. 5B**), while the remaining 11 perturbations yielded
322 insignificant and/or inconsistent effects (**Fig. S11**). The RNA-seq data from these perturbations
323 did not cluster based on proliferation phenotype (**Fig. S12**), suggesting that phenotypic effects
324 for processes such as proliferation may be difficult to predict from RNA-seq data alone, and
325 underscoring the importance of experimental analysis of such phenotypes.
326

327 Disruption of ASD Genes and Adjacent lncRNAs Alters Cerebral Organoid Development

328 Inducible KD in cerebral organoids further revealed shared neurodevelopmental phenotypes
329 in a complex model system. We created the FLEx-based Inducible CRISPR Knockdown
330 (FLICK) construct by engineering several features into a backbone incorporating the FLEx
331 design (Schnütgen et al. 2003). Ultimately, the FLICK construct enables control over the timing
332 of KD through doxycycline-inducible genetic recombination that results in the constitutive
333 expression of Cas13 and an EGFP reporter (**Fig. 5C**), and this was confirmed to provide strong
334 KD (**Fig. S13A**). The FLICK constructs also contained identifying (ID) sequences that can be
335 captured during scRNA-seq and used to determine the KD target in a given cell, enabling the
336 analysis of mosaic cerebral organoids. For long-term studies, we targeted ASD genes and
337 adjacent lncRNAs whose KDs had not been found to impair NPC proliferation (**Fig. 5B** and **Fig.
338 S11**) or survival (not shown). FLICK constructs targeting these various genes were separately
339 transposed into iPSCs, and subsequently the cells were pooled to generate mosaic organoids
340 (d0). KD was induced by one day of treatment with doxycycline on d14-15, when the organoids
341 predominantly consist of PAX6+ NPCs (**Fig. S13B**). The organoids were grown until they
342 reached one or two months of development (**Fig. 5D**), at which point analysis through scRNA-
343 seq enabled the identification of multiple cell types including radial glial progenitors (RGs),
344 intermediate progenitor cells (IPCs), excitatory neurons (ExNs), and inhibitory neurons (INs)
345 (**Fig. 5E-F** and **Fig. S13C-D**).

346 These long-term organoid KDs revealed shared changes in cell type composition across
347 multiple perturbations. Cells with FLICK constructs targeting the SFARI genes *BAZ2B*, *CLASP1*,
348 and *EHMT1* as well as the lncRNA *ST7-AS1* appeared relatively depleted from the organoids at
349 both d30 and d60 (**Fig. 6A**), despite our previous finding that these KDs did not impair NPC
350 proliferation or survival (**Fig. 5B** and **Fig. S11**). Furthermore, these KDs also altered cell type
351 proportions, leading to relatively more ExNs and fewer RGs (**Fig. 6B**). Together, this suggests
352 that disruption of these genes may result in increased ExN differentiation at the expense of RG

353 self-renewal, leading to an overall reduction in cell number in the developing organoids.
354 Additionally, several other KDs appeared to result in an increased proportion of ExNs by the 2-
355 month timepoint, including the SFARI genes *PPP3CA* and *WDFY3* as well as the lncRNAs
356 *NR2F1-AS1* and *WDFY3-AS2*. Thus, the disruption of multiple different ASD genes and
357 neighboring lncRNAs results in this convergent neurodevelopmental phenotype, consistent with
358 previous observations (Paulsen et al. 2022; Jourdon et al. 2023).
359 Furthermore, depletion of ASD genes and adjacent lncRNAs resulted in prominent
360 transcriptomic convergence (**Fig. 6C** and **S14A**). Effects on gene expression were analyzed for
361 each major cell type, which revealed highly overlapping DEGs in RGs with different KDs, further
362 supporting our previous findings from NPC cultures. Indeed, for many of the KD targets, the
363 DEGs that resulted from KD in organoid RGs strongly overlapped with the DEGs that we had
364 previously identified from NPC cultures (**Fig. S14B**), suggesting that these effects on gene
365 expression are not specific to a particular model system. Furthermore, strongly overlapping
366 DEGs were also observed within additional cell types including ExNs (**Fig. 6C**) and IPCs (**Fig.
367 S14A**), demonstrating that the convergence of ASD genes on shared downstream effects is not
368 unique to neural progenitors. However, some of the specific genes that were convergently
369 disrupted across perturbations differed between cell types, even when only considering genes
370 expressed in all of the cell types (**Fig. 6D**), suggesting that cell-type-specific features impact the
371 transcriptomic consequences of perturbing ASD genes. Additionally, down-sampling analysis
372 revealed that the detection of overlapping DEGs heavily depended upon the number of cells
373 sequenced for each perturbation (**Fig. S14C**). This demonstrates that strong transcriptomic
374 convergence cannot be detected unless sufficiently large numbers of cells are analyzed.
375 Several ASD gene and adjacent lncRNA perturbations resulted in DEGs that were enriched
376 for other ASD-relevant gene sets, including SFARI genes (**Fig. S14D**). This enrichment was
377 observed across multiple cell types at both the d30 and d60 timepoints, further demonstrating
378 that disruption of a single target gene can lead to broad dysregulation of many ASD genes.

379 Furthermore, shared DEGs implicated key transcriptional regulators as potential drivers of
380 transcriptomic convergence. Analysis using the bioinformatics tool MAGIC (Roopra 2020)
381 identified regulators whose putative target genes were disrupted by several of the perturbations
382 (**Fig. 6E** and **Fig. S15**). Of the top 25 recurrent regulators identified from the RGs of 1-month
383 organoids (**Fig. S15**), over half (14/25, 56%) overlapped with the top recurrent MAGIC TFs that
384 we had previously identified from NPCs (**Fig. 2D**). Moreover, this analysis revealed recurrent
385 regulators in ExNs from 1-month and 2-month organoids (**Fig. S15**), 21 of which were shared by
386 ExNs from both timepoints. This set contained several SFARI genes (5/21, 23.8%), including
387 CHD family members *CHD1* and *CHD7* (*CHD8* is not analyzed by MAGIC due to lack of
388 ENCODE data at the time of MAGIC's creation). It also contained multiple genes that had been
389 identified as top candidate regulators through previous GRN analysis (5/21, 23.8%) including
390 *REST*. Interestingly, ten regulators including *REST* were also shared with the 1-month RGs,
391 suggesting that these regulators are important drivers of convergence in multiple cellular
392 contexts.
393
394 <u>Transcriptomic Convergence is Further Revealed by Acute Perturbations in Cerebral Organoids</u>
395 Acute disruption of ASD genes and adjacent lncRNAs in 2-month organoids revealed even
396 greater convergence on shared DEGs. We allowed an additional set of mosaic FLICK organoids
397 to grow for two months prior to inducing KD by treatment with doxycycline at d61-d62 and
398 performing scRNA-seq two days later, allowing us to determine the acute effects of disrupting
399 these genes within organoids that had developed normally. This approach resulted in similar
400 numbers of cells with each of the different KDs (**Fig. 7A** and **S16A**), enabling deeper analysis of
401 the KDs that had been depleted from the organoids with long-term KD (**Fig. 6A**). These
402 organoids contained a mixture of cell types including RGs, IPCs, and ExNs (**Fig. 7B** and **Fig.
403 S15B-C**); however, we focused on ExNs, as they were by far the most abundant cell type at this
404 timepoint. Interestingly, when limiting our analysis to genes that are expressed in both the

405 organoid ExNs and our earlier NPC cultures, many of the KDs resulted in ExN DEGs that were
406 enriched for the NPC DEGs that we had previously identified (**Fig. 7C**). While there are certainly
407 cell-type-specific effects of the different KDs, this demonstrates that there are also shared
408 changes in gene expression across cell types that can be partially modeled in experimentally
409 tractable NPC cultures.

410 Furthermore, for perturbations that had been depleted from organoids over long-term KD,
411 acute KD enabled us to obtain much greater cell numbers, revealing that these KDs similarly
412 resulted in transcriptomic convergence (**Fig. 7D** and **S16D-E**). The DEGs exhibited strong
413 enrichment of ASD-relevant genes, including SFARI genes, across several of the perturbations
414 (**Fig. S16F**). Analysis of transcriptional regulators through MAGIC (Roopra 2020) identified 31
415 transcription factors and co-factors whose targets were enriched within the DEGs from at least
416 half of the perturbations (**Fig. 7E**). These included 8/10 (80%) of the top regulators that had
417 previously been identified in all three analyses from the long-term organoid KDs (1-month RGs,
418 1-month ExNs, and 2-month ExNs). Moreover, seven of these regulators, including *REST*, had
419 also been identified as top recurrent MAGIC TFs from the previous NPC studies (**Fig. 2D**),
420 further suggesting that they are key drivers of transcriptomic convergence in multiple cellular
421 contexts and across acute and long-term time scales. Together, these studies reveal ASD
422 genes and neighboring lncRNAs whose disruptions result in convergent effects on ASD gene
423 expression as well as shared neurodevelopmental phenotypes in NPCs and cerebral organoids.
424

425 **DISCUSSION**

426 Here, we present several functional studies of ASD genes and neighboring lncRNAs in
427 human NPCs and cerebral organoids, which demonstrated strong transcriptomic convergence
428 including widespread dysregulation of ASD genes. GRN analysis revealed regulatory
429 relationships that highlighted key chromatin modifiers and transcription factors, including *CHD8*
430 and *REST*, as critical drivers of transcriptomic convergence. These regulators were highly

431 interconnected, with many demonstrating mutual regulation of one another, revealing how
432 disruption of a single regulator can lead to changes that propagate throughout the network.
433 Furthermore, the X-linked transcription factor *ZFX* was identified as a key contributor to the
434 female protective effect through its female-biased expression and transcriptional activation of
435 ASD-associated genes, which could buffer the effects of disrupting these genes in females.
436 More broadly, this highlights a role for the "inactive" X chromosome in potentially mediating sex
437 differences in ASD. Several ASD gene or neighboring lncRNA perturbations also altered NPC
438 proliferation, demonstrating that these disruptions can result in shared phenotypic effects.
439 Moreover, several KDs in cerebral organoids led to altered cell type proportions, resulting in a
440 relative increase in ExNs. Thus, this work revealed critical insights into how diverse genes,
441 including lncRNAs, can converge on core transcriptomic changes and neurodevelopmental
442 phenotypes, ultimately resulting in ASD.

443 To uncover transcriptomic convergence, we initially focused on functional studies of ASD
444 genes and neighboring lncRNAs in highly homogeneous human NPC cultures. This enabled
445 bulk RNA-seq of each perturbation, providing the deep transcriptomic data that was essential for
446 robust GRN reconstruction. Building an understanding of the complex relationships within GRNs
447 is critical for identifying key "rate-limiting" factors that affect the GRN as a whole and ultimately
448 lead to a particular biological outcome (Chakravarti and Turner 2016). For instance, studies of
449 Hirschsprung disease have identified a crucial GRN centered on the rate-limiting gene *RET* that
450 can be impacted by direct mutations in *RET* itself or in upstream regulators of *RET* (Chatterjee
451 et al. 2016). Here, we have similarly identified critical genes such as *CHD8* and *REST* whose
452 effects can propagate throughout the GRN, driving transcriptomic convergence in ASD.

453 While some of the specific regulatory relationships uncovered here may be unique to NPCs,
454 our subsequent studies in cerebral organoids implicated several of these regulators in ExNs as
455 well. Furthermore, the organoid analyses demonstrated that ExNs also exhibit convergence of
456 ASD genes on shared downstream targets. Thus, future studies to reconstruct GRNs from

457 additional cell types including ExNs will be highly valuable for understanding how regulatory
458 relationships are reorganized in different cellular contexts. While bioinformatic pipelines for
459 reconstructing GRNs from scRNA-seq data are actively being refined (Vlahos et al. 2021;
460 Obradovic et al. 2021), these approaches are currently hampered by limited RNA capture
461 inherent to the scRNA-seq techniques. As these continue to improve, it will be feasible to
462 reconstruct robust GRNs from heterogeneous models, including organoids, as well as patient
463 tissue samples, which will further refine our understanding of gene regulation in complex
464 biological systems.

465 This study also identified several lncRNAs that affect the expression of their ASD gene
466 neighbor or other ASD genes more broadly. Intriguingly, the transcriptomic changes resulting
467 from the lncRNA KDs in NPCs were highly correlated with those from the KD of their ASD gene
468 neighbors, though the lncRNAs generally had milder effects, consistent with previous findings
469 that lncRNAs tend to be more subtle modulators of gene expression (Gao et al. 2020). This was
470 also the case for *NR2F1-AS1* (Ang et al. 2019) and *SOX2-OT* (Andersen et al. 2024), lncRNAs
471 that have been directly implicated in ASD. Thus, these lncRNAs may play neurodevelopmental
472 roles through their effects on ASD genes, providing context to previous findings that many
473 lncRNAs are dysregulated in ASD (Parikshak et al. 2016). Importantly, lncRNAs have often
474 been excluded or overlooked in genetic studies (Mattick et al. 2023), and these findings
475 highlight the value of especially careful consideration of lncRNAs that closely neighbor known
476 critical genes.

477 Taken together, these results have broad implications for our understanding of
478 neurodevelopment and disorders such as ASD. In particular, this work identified several
479 regulators that drive transcriptomic convergence, including the prominent ASD gene *CHD8* as
480 well as candidates including *REST*. While *REST* has not been directly implicated in ASD,
481 individuals with ASD exhibit decreased expression of *REST* targets (Katayama et al. 2016), and
482 treatment with a *REST* inhibitor can ameliorate deficits in social interaction in a valproic acid

483 mouse model of ASD (Kawase et al. 2019). Our findings further support that *REST* is a critical
484 regulator of ASD-associated gene expression and suggest a general paradigm for identifying
485 regulators of transcriptomic changes in ASD that may ultimately suggest new therapeutic
486 targets. More broadly, while this work focused on ASD, the approaches used here are widely
487 applicable to different cell types and conditions. Thus, this study serves as a framework for
488 uncovering critical regulators across a wide diversity of contexts, from development through
489 disease.

490 **ACKNOWLEDGEMENTS**

491 We thank members of the Walsh Lab for helpful discussions. We are also grateful to Dr. August
492 Yue Huang for technical feedback regarding statistical analyses, and to Dr. Adrianna San
493 Roman and Dr. Marla Tharp of the Page Lab for their insights regarding the role of *ZFX*. This
494 work was facilitated by the BCH Flow Cytometry Research Core, the BCH IDDRC Molecular
495 Genetics Core Facility, the BCH Cellular Imaging Core, and Lingsheng Dong of the HMS
496 Research Computing Core. This project was supported by Autism Speaks Postdoctoral
497 Fellowship 13008 and NIGMS T32 GM007748 (R.E.A.); T32 GM007753 and T32 GM144273
498 (M.T.); the Harvard Program for Research in Science and Engineering and the Harvard College
499 Research Program (T.S.); a Howard Hughes Medical Institute Fellowship from the Helen Hay
500 Whitney Foundation and Grant K99MH136290 from NIMH/NIH (J.H.T.S); K99 NS135123 from
501 the NINDS/NIH (X.Q.); the Howard Hughes Medical Institute and Grant K99EY034603 from
502 NEI/NIH (R.N.D); the Harvard-Amgen Scholars Program (G.E.); and grants from the Simons
503 Foundation and Autism BrainNet (953759), NIMH (U01MH106883), the Hock E. Tan and K. Lisa
504 Yang Center for Autism Research at Harvard University, and the Allen Discovery Center
505 program, a Paul G. Allen Frontiers Group advised program of the Paul G. Allen Family
506 Foundation (C.A.W). C.A.W. is an investigator of the Howard Hughes Medical Institute.

507 **REFERENCES**

508 Abrahams BS, Arking DE, Campbell DB, et al (2013) SFARI Gene 2.0: a community-driven
509 knowledgebase for the autism spectrum disorders (ASDs). Mol Autism 4:36.
510 https://doi.org/10.1186/2040-2392-4-36
511 Alvarez MJ, Shen Y, Giorgi FM, et al (2016) Functional characterization of somatic mutations in
512 cancer using network-based inference of protein activity. Nat Genet 48:838–47.
513 https://doi.org/10.1038/ng.3593
514 Andersen RE, Alkuraya IF, Ajeesh A, et al (2024) Chromosomal structural rearrangements
515 implicate long non-coding RNAs in rare germline disorders. Hum Genet 143:921–938.
516 https://doi.org/10.1007/s00439-024-02693-y
517 Ang CE, Ma Q, Wapinski OL, et al (2019) The novel lncRNA lnc-NR2F1 is pro-neurogenic and
518 mutated in human neurodevelopmental disorders. Elife 8:.
519 https://doi.org/10.7554/eLife.41770
520 Antaki D, Guevara J, Maihofer AX, et al (2022) A phenotypic spectrum of autism is attributable
521 to the combined effects of rare variants, polygenic risk and sex. Nat Genet 54:1284–1292.
522 https://doi.org/10.1038/s41588-022-01064-5
523 Bai D, Yip BHK, Windham GC, et al (2019) Association of Genetic and Environmental Factors
524 With Autism in a 5-Country Cohort. JAMA Psychiatry 76:1035.
525 https://doi.org/10.1001/jamapsychiatry.2019.1411
526 Blanton L V, San Roman AK, Wood G, et al (2024) Stable and robust Xi and Y transcriptomes
527 drive cell-type-specific autosomal and Xa responses in vivo and in vitro in four human cell
528 types. Cell genomics 4:100628. https://doi.org/10.1016/j.xgen.2024.100628
529 Boukas L, Havrilla JM, Hickey PF, et al (2019) Coexpression patterns define epigenetic
530 regulators associated with neurological dysfunction. Genome Res 29:532–542.
531 https://doi.org/10.1101/gr.239442.118
532 Chakravarti A, Turner TN (2016) Revealing rate-limiting steps in complex disease biology: The
533 crucial importance of studying rare, extreme-phenotype families. Bioessays 38:578–86.
534 https://doi.org/10.1002/bies.201500203
535 Chatterjee S, Kapoor A, Akiyama JA, et al (2016) Enhancer Variants Synergistically Drive
536 Dysfunction of a Gene Regulatory Network In Hirschsprung Disease. Cell 167:355-
537 368.e10. https://doi.org/10.1016/j.cell.2016.09.005
538 Chong JA, Tapia-Ramírez J, Kim S, et al (1995) REST: a mammalian silencer protein that
539 restricts sodium channel gene expression to neurons. Cell 80:949–57.
540 https://doi.org/10.1016/0092-8674(95)90298-8
541 Connacher R, Williams M, Prem S, et al (2022) Autism NPCs from both idiopathic and CNV
542 16p11.2 deletion patients exhibit dysregulation of proliferation and mitogenic responses.
543 Stem Cell Reports 17:1380–1394. https://doi.org/10.1016/j.stemcr.2022.04.019
544 Dias CM, Walsh CA (2020) Recent Advances in Understanding the Genetic Architecture of
545 Autism. Annu Rev Genomics Hum Genet 21:289–304. https://doi.org/10.1146/annurev-
546 genom-121219-082309
547 Dougherty JD, Marrus N, Maloney SE, et al (2022) Can the "female protective effect"
548 liability threshold model explain sex differences in autism spectrum disorder? Neuron
549 110:3243–3262. https://doi.org/10.1016/j.neuron.2022.06.020
550 Gandal MJ, Haney JR, Wamsley B, et al (2022) Broad transcriptomic dysregulation occurs
551 across the cerebral cortex in ASD. Nature 611:532–539. https://doi.org/10.1038/s41586-
552 022-05377-7
553 Gao F, Cai Y, Kapranov P, Xu D (2020) Reverse-genetics studies of lncRNAs—what we have
554 learnt and paths forward. Genome Biol 21:93. https://doi.org/10.1186/s13059-020-01994-5
555 Graham V, Khudyakov J, Ellis P, Pevny L (2003) SOX2 functions to maintain neural progenitor
556 identity. Neuron 39:749–65. https://doi.org/10.1016/s0896-6273(03)00497-5

557 Grove J, Ripke S, Als TD, et al (2019) Identification of common genetic risk variants for autism
558 spectrum disorder. Nat Genet 51:431–444. https://doi.org/10.1038/s41588-019-0344-8
559 Haddad Derafshi B, Danko T, Chanda S, et al (2022) The autism risk factor CHD8 is a
560 chromatin activator in human neurons and functionally dependent on the ERK-MAPK
561 pathway effector ELK1. Sci Rep 12:22425. https://doi.org/10.1038/s41598-022-23614-x
562 Iakoucheva LM, Muotri AR, Sebat J (2019) Getting to the Cores of Autism. Cell 178:1287–1298.
563 https://doi.org/10.1016/j.cell.2019.07.037
564 Jacquemont S, Coe BP, Hersch M, et al (2014) A higher mutational burden in females supports
565 a "female protective model" in neurodevelopmental disorders. Am J Hum Genet
566 94:415–25. https://doi.org/10.1016/j.ajhg.2014.02.001
567 Jourdon A, Wu F, Mariani J, et al (2023) Modeling idiopathic autism in forebrain organoids
568 reveals an imbalance of excitatory cortical neuron subtypes during early neurogenesis. Nat
569 Neurosci 26:1505–1515. https://doi.org/10.1038/s41593-023-01399-0
570 Kalkman H (2012) A review of the evidence for the canonical Wnt pathway in autism spectrum
571 disorders. Mol Autism 3:10. https://doi.org/10.1186/2040-2392-3-10
572 Katayama Y, Nishiyama M, Shoji H, et al (2016) CHD8 haploinsufficiency results in autistic-like
573 phenotypes in mice. Nature 537:675–679. https://doi.org/10.1038/nature19357
574 Kawase H, Ago Y, Naito M, et al (2019) mS-11, a mimetic of the mSin3-binding helix in NRSF,
575 ameliorates social interaction deficits in a prenatal valproic acid-induced autism mouse
576 model. Pharmacol Biochem Behav 176:1–5. https://doi.org/10.1016/j.pbb.2018.11.003
577 Kissel LT, Pochareddy S, An J-Y, et al (2024) Sex-Differential Gene Expression in Developing
578 Human Cortex and Its Intersection With Autism Risk Pathways. Biological psychiatry global
579 open science 4:100321. https://doi.org/10.1016/j.bpsgos.2024.100321
580 Kochinke K, Zweier C, Nijhof B, et al (2016) Systematic Phenomics Analysis Deconvolutes
581 Genes Mutated in Intellectual Disability into Biologically Coherent Modules. Am J Hum
582 Genet 98:149–64. https://doi.org/10.1016/j.ajhg.2015.11.024
583 Konermann S, Lotfy P, Brideau NJ, et al (2018) Transcriptome Engineering with RNA-Targeting
584 Type VI-D CRISPR Effectors. Cell 173:665-676.e14.
585 https://doi.org/10.1016/j.cell.2018.02.033
586 Kostyanovskaya E, Lasser MC, Wang B, et al (2025) Convergence of autism proteins at the
587 cilium. bioRxiv. https://doi.org/10.1101/2024.12.05.626924
588 Lachmann A, Giorgi FM, Lopez G, Califano A (2016) ARACNe-AP: gene network reverse
589 engineering through adaptive partitioning inference of mutual information. Bioinformatics
590 32:2233–2235. https://doi.org/10.1093/bioinformatics/btw216
591 Lambert SA, Jolma A, Campitelli LF, et al (2018) The Human Transcription Factors. Cell
592 172:650–665. https://doi.org/10.1016/J.CELL.2018.01.029
593 Lasser M, Sun N, Xu Y, et al (2023) Pleiotropy of autism-associated chromatin regulators.
594 Development 150:dev201515. https://doi.org/10.1242/dev.201515
595 Lee KE, Seo J, Shin J, et al (2014) Positive feedback loop between Sox2 and Sox6 inhibits
596 neuronal differentiation in the developing central nervous system. Proc Natl Acad Sci U S A
597 111:2794–9. https://doi.org/10.1073/pnas.1308758111
598 Lek M, Karczewski KJ, Minikel E V., et al (2016) Analysis of protein-coding genetic variation in
599 60,706 humans. Nature 536:285–291. https://doi.org/10.1038/nature19057
600 Li C, Fleck JS, Martins-Costa C, et al (2023) Single-cell brain organoid screening identifies
601 developmental defects in autism. Nature 621:373–380. https://doi.org/10.1038/s41586-023-
602 06473-y
603 Liao C, Moyses-Oliveira M, De Esch CEF, et al (2023) Convergent coexpression of autism-
604 associated genes suggests some novel risk genes may not be detectable in large-scale
605 genetic studies. Cell Genomics 3:100277. https://doi.org/10.1016/j.xgen.2023.100277

606 Loomes R, Hull L, Mandy WPL (2017) What Is the Male-to-Female Ratio in Autism Spectrum
607 Disorder? A Systematic Review and Meta-Analysis. J Am Acad Child Adolesc Psychiatry
608 56:466–474. https://doi.org/10.1016/j.jaac.2017.03.013
609 Luo S, Lu JY, Liu L, et al (2016) Divergent lncRNAs Regulate Gene Expression and Lineage
610 Differentiation in Pluripotent Cells. Cell Stem Cell 18:637–652.
611 https://doi.org/10.1016/j.stem.2016.01.024
612 Luo T, Liu P, Wang X-Y, et al (2018) Effect of the autism-associated lncRNA Shank2-AS on
613 architecture and growth of neurons. J Cell Biochem. https://doi.org/10.1002/jcb.27471
614 Maenner MJ, Warren Z, Williams AR, et al (2023) Prevalence and Characteristics of Autism
615 Spectrum Disorder Among Children Aged 8 Years - Autism and Developmental Disabilities
616 Monitoring Network, 11 Sites, United States, 2020. MMWR Surveill Summ 72:1–14.
617 https://doi.org/10.15585/mmwr.ss7202a1
618 Margolin AA, Nemenman I, Basso K, et al (2006) ARACNE: an algorithm for the reconstruction
619 of gene regulatory networks in a mammalian cellular context. BMC Bioinformatics 7 Suppl
620 1:S7. https://doi.org/10.1186/1471-2105-7-S1-S7
621 Martin HC, Gardner EJ, Samocha KE, et al (2021) The contribution of X-linked coding variation
622 to severe developmental disorders. Nat Commun 12:627. https://doi.org/10.1038/s41467-
623 020-20852-3
624 Mattick JS, Amaral PP, Carninci P, et al (2023) Long non-coding RNAs: definitions, functions,
625 challenges and recommendations. Nat Rev Mol Cell Biol 24:430–447.
626 https://doi.org/10.1038/s41580-022-00566-8
627 Mendes M, Chen DZ, Engchuan W, et al (2024) Chromosome X-wide common variant
628 association study in autism spectrum disorder. Am J Hum Genet 0:
629 https://doi.org/10.1016/j.ajhg.2024.11.008
630 Napolitano A, Schiavi S, La Rosa P, et al (2022) Sex Differences in Autism Spectrum Disorder:
631 Diagnostic, Neurobiological, and Behavioral Features. Front Psychiatry 13:889636.
632 https://doi.org/10.3389/fpsyt.2022.889636
633 Noor A, Whibley A, Marshall CR, et al (2010) Disruption at the PTCHD1 Locus on Xp22.11 in
634 Autism spectrum disorder and intellectual disability. Sci Transl Med 2:49ra68.
635 https://doi.org/10.1126/scitranslmed.3001267
636 Obradovic A, Chowdhury N, Haake SM, et al (2021) Single-cell protein activity analysis
637 identifies recurrence-associated renal tumor macrophages. Cell 184:2988-3005.e16.
638 https://doi.org/10.1016/J.CELL.2021.04.038
639 Oliva M, Muñoz-Aguirre M, Kim-Hellmuth S, et al (2020) The impact of sex on gene expression
640 across human tissues. Science 369:. https://doi.org/10.1126/science.aba3066
641 Page L, Brin S, Motwani R, Winograd T (1999) The PageRank Citation Ranking : Bringing Order
642 to the Web. The Web Conference
643 Parikshak NN, Swarup V, Belgard TG, et al (2016) Genome-wide changes in lncRNA, splicing,
644 and regional gene expression patterns in autism. Nature 540:423–427.
645 https://doi.org/10.1038/nature20612
646 Paulsen B, Velasco S, Kedaigle AJ, et al (2022) Autism genes converge on asynchronous
647 development of shared neuron classes. Nature 602:268–273.
648 https://doi.org/10.1038/s41586-021-04358-6
649 Pinto D, Delaby E, Merico D, et al (2014) Convergence of genes and cellular pathways
650 dysregulated in autism spectrum disorders. Am J Hum Genet 94:677–94.
651 https://doi.org/10.1016/j.ajhg.2014.03.018
652 Price E, Fedida LM, Pugacheva EM, et al (2023) An updated catalog of CTCF variants
653 associated with neurodevelopmental disorder phenotypes. Front Mol Neurosci 16:1185796.
654 https://doi.org/10.3389/fnmol.2023.1185796

655 Ramaswami G, Won H, Gandal MJ, et al (2020) Integrative genomics identifies a convergent
656 molecular subtype that links epigenomic with transcriptomic differences in autism. Nat
657 Commun 11:4873. https://doi.org/10.1038/s41467-020-18526-1
658 Raznahan A, Parikshak NN, Chandran V, et al (2018) Sex-chromosome dosage effects on gene
659 expression in humans. Proc Natl Acad Sci U S A 115:7398–7403.
660 https://doi.org/10.1073/pnas.1802889115
661 Rhie SK, Yao L, Luo Z, et al (2018) ZFX acts as a transcriptional activator in multiple types of
662 human tumors by binding downstream from transcription start sites at the majority of CpG
663 island promoters. Genome Res 28:310–320. https://doi.org/10.1101/gr.228809.117
664 Rockowitz S, Zheng D (2015) Significant expansion of the REST/NRSF cistrome in human
665 versus mouse embryonic stem cells: potential implications for neural development. Nucleic
666 Acids Res 43:5730–43. https://doi.org/10.1093/nar/gkv514
667 Roopra A (2020) MAGIC: A tool for predicting transcription factors and cofactors driving gene
668 sets using ENCODE data. PLoS Comput Biol 16:e1007800.
669 https://doi.org/10.1371/journal.pcbi.1007800
670 Ropers H-H, Hamel BCJ (2005) X-linked mental retardation. Nat Rev Genet 6:46–57.
671 https://doi.org/10.1038/nrg1501
672 San Roman AK, Godfrey AK, Skaletsky H, et al (2023) The human inactive X chromosome
673 modulates expression of the active X chromosome. Cell genomics 3:100259.
674 https://doi.org/10.1016/j.xgen.2023.100259
675 San Roman AK, Skaletsky H, Godfrey AK, et al (2024) The human Y and inactive X
676 chromosomes similarly modulate autosomal gene expression. Cell genomics 4:100462.
677 https://doi.org/10.1016/j.xgen.2023.100462
678 Satterstrom FK, Kosmicki JA, Wang J, et al (2020) Large-Scale Exome Sequencing Study
679 Implicates Both Developmental and Functional Changes in the Neurobiology of Autism
680 Article Large-Scale Exome Sequencing Study Implicates Both Developmental and
681 Functional Changes in the Neurobiology of Autism. Cell 1–17.
682 https://doi.org/10.1016/j.cell.2019.12.036
683 Schnütgen F, Doerflinger N, Calléja C, et al (2003) A directional strategy for monitoring Cre-
684 mediated recombination at the cellular level in the mouse. Nat Biotechnol 21:562–5.
685 https://doi.org/10.1038/nbt811
686 Schoenherr CJ, Anderson DJ (1995) The neuron-restrictive silencer factor (NRSF): a coordinate
687 repressor of multiple neuron-specific genes. Science 267:1360–3.
688 https://doi.org/10.1126/science.7871435
689 Shepherdson JL, Hutchison K, Don DW, et al (2024) Variants in ZFX are associated with an X-
690 linked neurodevelopmental disorder with recurrent facial gestalt. Am J Hum Genet
691 111:487–508. https://doi.org/10.1016/j.ajhg.2024.01.007
692 Subramanian A, Tamayo P, Mootha VK, et al (2005) Gene set enrichment analysis: A
693 knowledge-based approach for interpreting genome-wide expression profiles. Proceedings
694 of the National Academy of Sciences 102:15545–15550.
695 https://doi.org/10.1073/pnas.0506580102
696 Sugathan A, Biagioli M, Golzio C, et al (2014) CHD8 regulates neurodevelopmental pathways
697 associated with autism spectrum disorder in neural progenitors. Proc Natl Acad Sci U S A
698 111:E4468-77. https://doi.org/10.1073/pnas.1405266111
699 Sun N, Teyssier N, Wang B, et al (2024) Autism genes converge on microtubule biology and
700 RNA-binding proteins during excitatory neurogenesis. bioRxiv.
701 https://doi.org/10.1101/2023.12.22.573108
702 Szklarczyk D, Kirsch R, Koutrouli M, et al (2023) The STRING database in 2023: protein-protein
703 association networks and functional enrichment analyses for any sequenced genome of
704 interest. Nucleic Acids Res 51:D638–D646. https://doi.org/10.1093/nar/gkac1000

Trost B, Thiruvahindrapuram B, Chan AJS, et al (2022) Genomic architecture of autism from comprehensive whole-genome sequence annotation. Cell 185:4409-4427.e18. https://doi.org/10.1016/j.cell.2022.10.009

Valencia AM, Sankar A, van der Sluijs PJ, et al (2023) Landscape of mSWI/SNF chromatin remodeling complex perturbations in neurodevelopmental disorders. Nat Genet 55:1400–1412. https://doi.org/10.1038/s41588-023-01451-6

Velmeshev D, Perez Y, Yan Z, et al (2023) Single-cell analysis of prenatal and postnatal human cortical development. Science (1979) 382:. https://doi.org/10.1126/science.adf0834

Villegas VE, Zaphiropoulos PG (2015) Neighboring gene regulation by antisense long non-coding RNAs. Int J Mol Sci 16:3251–66. https://doi.org/10.3390/ijms16023251

Vlahos L, Obradovic A, Worley J, et al (2021) Systematic, Protein Activity-based Characterization of Single Cell State. bioRxiv 2021.05.20.445002

Voineagu I, Wang X, Johnston P, et al (2011) Transcriptomic analysis of autistic brain reveals convergent molecular pathology. Nature 474:380–4. https://doi.org/10.1038/nature10110

Wang Y, Chen S, Li W, et al (2020) Associating divergent lncRNAs with target genes by integrating genome sequence, gene expression and chromatin accessibility data. NAR Genom Bioinform 2:lqaa019. https://doi.org/10.1093/nargab/lqaa019

Warrier V, Zhang X, Reed P, et al (2022) Genetic correlates of phenotypic heterogeneity in autism. Nat Genet 54:1293–1304. https://doi.org/10.1038/s41588-022-01072-5

Wei J, Lotfy P, Faizi K, et al (2023) Deep learning and CRISPR-Cas13d ortholog discovery for optimized RNA targeting. Cell Syst 14:1087-1102.e13. https://doi.org/10.1016/j.cels.2023.11.006

Weinschutz Mendes H, Neelakantan U, Liu Y, et al (2023) High-throughput functional analysis of autism genes in zebrafish identifies convergence in dopaminergic and neuroimmune pathways. Cell Rep 42:112243. https://doi.org/10.1016/j.celrep.2023.112243

Wenderski W, Wang L, Krokhotin A, et al (2020) Loss of the neural-specific BAF subunit ACTL6B relieves repression of early response genes and causes recessive autism. Proc Natl Acad Sci U S A 117:10055–10066. https://doi.org/10.1073/pnas.1908238117

Werling DM (2016) The role of sex-differential biology in risk for autism spectrum disorder. Biol Sex Differ 7:58. https://doi.org/10.1186/s13293-016-0112-8

Werling DM, Parikshak NN, Geschwind DH (2016) Gene expression in human brain implicates sexually dimorphic pathways in autism spectrum disorders. Nat Commun 7:10717. https://doi.org/10.1038/ncomms10717

Wigdor EM, Weiner DJ, Grove J, et al (2022) The female protective effect against autism spectrum disorder. Cell genomics 2:100134. https://doi.org/10.1016/j.xgen.2022.100134

Willsey HR, Willsey AJ, Wang B, State MW (2022) Genomics, convergent neuroscience and progress in understanding autism spectrum disorder. Nat Rev Neurosci 23:323–341. https://doi.org/10.1038/s41583-022-00576-7

Zhang Y, Li N, Li C, et al (2020) Genetic evidence of gender difference in autism spectrum disorder supports the female-protective effect. Transl Psychiatry 10:4. https://doi.org/10.1038/s41398-020-0699-8

Zhao S, Zhang X, Chen S, Zhang S (2021) Long noncoding RNAs: fine-tuners hidden in the cancer signaling network. Cell Death Discov 7:283. https://doi.org/10.1038/s41420-021-00678-8

Ziats MN, Rennert OM (2013) Aberrant expression of long noncoding RNAs in autistic brain. Journal of Molecular Neuroscience 49:589–593. https://doi.org/10.1007/s12031-012-9880-8

(2013) Diagnostic and statistical manual of mental disorders: DSM-5™, 5th ed. American Psychiatric Publishing, Inc., Arlington, VA, US

FIGURE LEGENDS

Figure 1

A) Schematic of the major classes of genetic variants within *Consensus-ASD*. **B)** Experimental design schematic. **C)** Immunocytochemistry of iPSC-derived NPC cultures. **D)** Relative expression of the targeted gene within each KD sample compared to non-targeting control (NTC) samples. Only targets with statistically significant KD are shown (see **Table S4**). Error bars: 95% confidence interval. KD target genes that have been directly implicated in ASD are labeled in bold text. **E)** Proportion of lncRNAs significantly differentially expressed upon KD of their neighboring PCG, and proportion of PCGs significantly differentially expressed upon KD of their neighboring lncRNA.

Figure 2

A) Bar plot depicting enrichment of *Consensus-ASD* genes within the DEGs of each KD condition. **B)** Circos plot depicting HC-SFARI DEGs shared between different KD conditions. **C)** Heatmap showing the relative expression of HC-SFARI genes that are DEGs in at least 5 KD conditions (see also **Fig. S5B**). Statistically significant DEGs are indicated with *. **D)** MAGIC analysis identifying transcriptional regulators whose targets are enriched within the DEGs from each KD (see also **Fig. S5C**). **E)** Bar plot depicting enrichment of REST targets within SFARI, *Consensus-ASD*, or SysID genes in human and mouse embryonic stem cells. REST target data from Rockowitz et al., 2015. Throughout the figure, KD target genes that have been directly implicated in ASD are labeled in bold text.

Figure 3

A) Volcano plot depicting differential expression upon KD of SETD5. Statistically significant DEGs with decreased expression are shown in blue, while DEGs with increased expression are shown in red. Genes within the 1st and 2nd degree SETD5 regulon, derived from an ARACNe

GRN constructed with SETD5 samples held out, are highlighted in pink. Genes within the 1st degree regulon are depicted with dark borders. Statistically significant enrichment of 1st and 2nd degree regulon genes within the downregulated DEGs is indicated with the adjusted p-value. **B)** Depiction of a subset of the NPC GRN constructed using ARACNE. All regulators are shown along with first degree target genes that are in *Consensus-ASD* or the HC-SFARI gene set. **C)** Gene set enrichment analysis (GSEA) demonstrating enrichment of genes ordered by PageRank score within several gene sets. **D)** Depiction of modules of top regulators identified through iterative walktrap clustering. Genes of particular interest are highlighted in red. **E)** Bar plot depicting enrichment of CHD8 targets within several gene categories. Data from CHD8 ChIP-seq in NPCs from Sugathan et al., 2014.

Figure 4

A) MAGIC analysis identifying X-linked transcriptional regulators whose targets are enriched within the DEGs from the NPC KDs. **B)** Binary heatmap of GRN-identified, X-linked regulators whose regulons are enriched for candidate ASD risk genes. Only target genes that are members of at least five of these aforementioned regulons are depicted. **C)** Network visualization of GRN-identified, X-linked regulators of candidate autism risk genes and their target genes. Edges directed to the top 20% most frequently targeted genes are depicted in black, and edges connecting two regulators are further bolded. All other edges are depicted in gray. Nodes representing SFARI genes are outlined in black. **D)** Heatmap showing the relative expression of *ZFX* upon KD of the indicated target genes. Statistically significant differential expression is indicated with *. **E)** Enrichment of gene sets relevant to autism and the female protective effect within *ZFX* targets identified from ChIP-seq and CRISPR KD experiments in San Roman et al., 2024. **F)** Depiction of the regulatory relationships between *ZFX* and target genes that are top drivers of transcriptomic convergence in ASD (previously identified in **Fig.**

3D). Throughout the figure, KD target genes that have been directly implicated in ASD are labeled in bold text.

Figure 5

A) Schematic of experimental design to analyze proliferation phenotypes using CytoTrack. **B)** Relative CytoTrack intensity over time for each KD condition that exhibited statistically significant proliferation phenotypes that were consistent over time. Error bars indicate standard error of the mean. Statistical significance was determined using 2-way ANOVA. See **Table S8** for full statistical results. KD target genes that have been directly implicated in ASD are labeled in bold text. **C)** Design of FLICK constructs for doxycycline-inducible Cas13 KD. **D)** Immunohistochemistry of FLICK organoid at day 60. EGFP = FLICK construct marker; PAX6 = NPC marker; TBR2 = intermediate progenitor cell marker; CTIP2 = excitatory neuron marker. **E)** UMAP of integrated organoid scRNA-seq data collected at d30 and d60. **F)** Expression of canonical brain marker genes used for identifying cell types.

Figure 6

A) Longitudinal analysis of the proportion of cells for each KD target in mosaic organoids in which the FLICK constructs were induced by treatment with doxycycline on d14-d15. KD targets that appear depleted over time are highlighted with arrows. **B)** Cell type composition per KD target. KD targets with fewer progenitors and an increased relative proportion of excitatory neurons are highlighted with arrows. **C)** Heatmap of cross-enrichment of DEGs for radial glia and excitatory neurons. **D)** Network visualization of DEGs amongst different KDs. The thickness of edges represents the number of shared DEGs. Nodes plotted based on clustering with the Fruchterman-Reingold algorithm (*igraph*). Nodes that are closer together have more shared DEGs on average. **E)** MAGIC analysis of DEGs from excitatory neurons (ExNs) in one-month

organoids (see also **Fig. S15**). Throughout the figure, KD target genes that have been directly implicated in ASD are labeled in bold text.

Figure 7

A) Proportion of cells with each KD target from scRNA-seq of mosaic organoids with acute KD. **B)** UMAP of acute KD mosaic organoids from scRNA-seq. **C)** Bar plot of cross-enrichment of DEGs from excitatory neurons (ExNs) from acute KD mosaic organoids versus DEGs from previous NPC cultures upon KD of the same target gene. **D)** Heatmap of cross-enrichment between different KD samples in ExNs. **E)** MAGIC analysis of ExN DEGs. Throughout the figure, KD target genes that have been directly implicated in ASD are labeled in bold text.

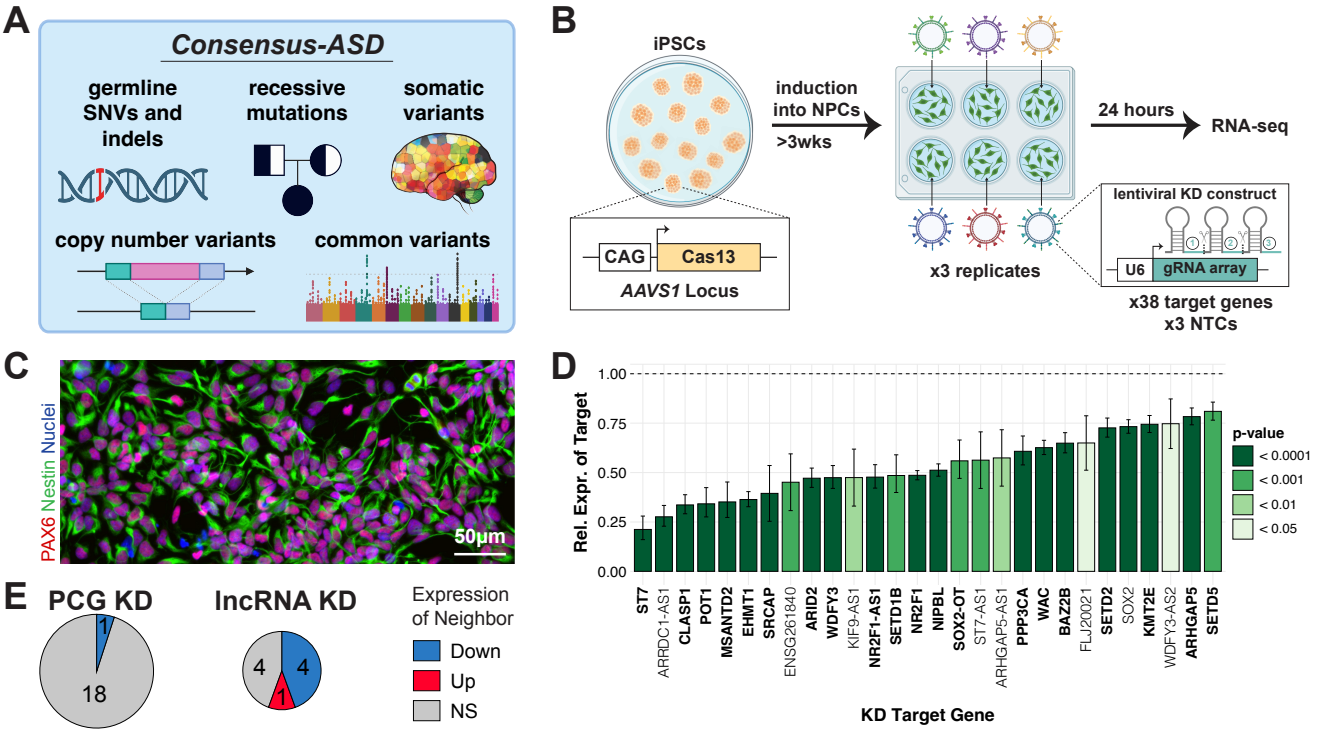
A
Consensus-ASD
germline SNVs and indels
recessive mutations
somatic variants
copy number variants
common variants
B
iPSCs
induction into NPCs
>3wks
24 hours
RNA-seq
CAG
Cas13
AAVS1 Locus
x3 replicates
lentiviral KD construct
U6
gRNA array
x38 target genes
x3 NTCs
C
PAX6 Nestin Nuclei
50µm
D
Rel. Expr. of Target
1.00
0.75
0.50
0.25
0.00
p-value
< 0.0001
< 0.001
< 0.01
< 0.05
ST7
ARRDC1-AS1
CLASP1
POT1
MSANTD2
EHMT1
SRCAP
ENSG261840
ARID2
WDFY3
KIF9-AS1
NR2F1-AS1
SETD1B
NR2F1
NIPBL
SOX2-OT
ST7-AS1
ARHGAP5-AS1
PPP3CA
WAC
BAZ2B
FLJ20021
SETD2
SOX2
KMT2E
WDFY3-AS2
ARHGAP5
SETD5
KD Target Gene
E
PCG KD
1
18
lncRNA KD
4
4
1
Expression of Neighbor
Down
Up
NS

Figure 1

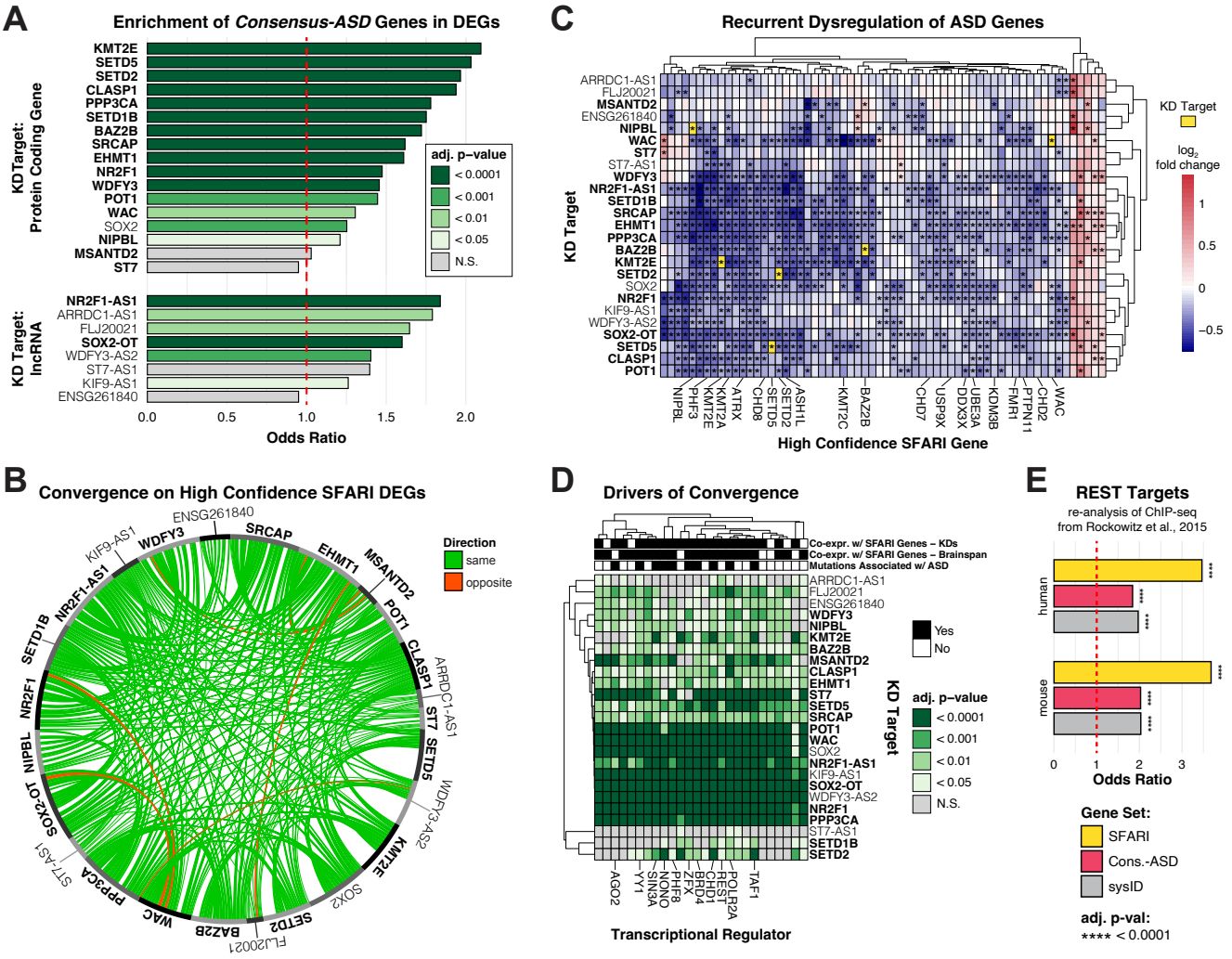
A
Enrichment of Consensus-ASD Genes in DEGs
KD Target: Protein Coding Gene
KMT2E
SETD5
SETD2
CLASP1
PPP3CA
SETD1B
BAZ2B
SRCAP
EHMT1
NR2F1
WDFY3
POT1
WAC
SOX2
NIPBL
MSANTD2
ST7
KD Target: lncRNA
NR2F1-AS1
ARRDC1-AS1
FLJ20021
SOX2-OT
WDFY3-AS2
ST7-AS1
KIF9-AS1
ENSG261840
adj. p-value
< 0.0001
< 0.001
< 0.01
< 0.05
N.S.
0.0
0.5
1.0
1.5
2.0
Odds Ratio
B
Convergence on High Confidence SFARI DEGs
Direction
same
opposite
C
Recurrent Dysregulation of ASD Genes
KD Target
log2 fold change
1
0.5
0
−0.5
NIPBL
PHF3
KMT2E
KMT2A
ATRX
CHD8
SETD5
SETD2
ASH1L
KMT2C
BAZ2B
CHD7
USP9X
DDX3X
UBE3A
KDM3B
FMR1
PTPN11
CHD2
WAC
High Confidence SFARI Gene
D
Drivers of Convergence
Co-expr. w/ SFARI Genes – KDs
Co-expr. w/ SFARI Genes – Brainspan
Mutations Associated w/ ASD
Yes
No
adj. p-value
< 0.0001
< 0.001
< 0.01
< 0.05
N.S.
AGO2
YY1
SIN3A
NONO
PHF8
ZFX
BRD4
CHD1
REST
POLR2A
TAF1
Transcriptional Regulator
E
REST Targets
re-analysis of ChIP-seq
from Rockowitz et al., 2015
human
mouse
0
1
2
3
Odds Ratio
Gene Set:
SFARI
Cons.-ASD
sysID
adj. p-val:
**** < 0.0001

Figure 2

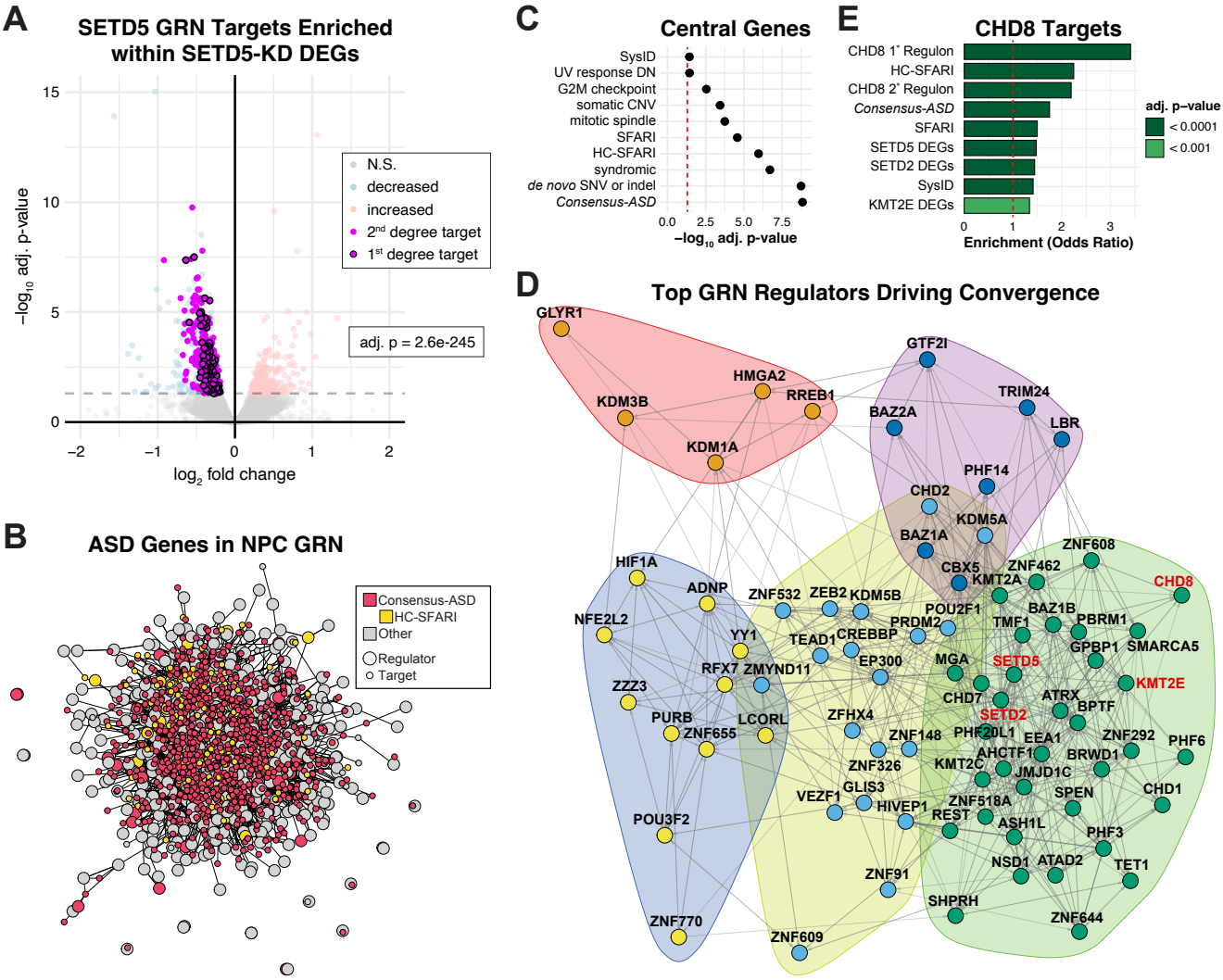
A
SETD5 GRN Targets Enriched within SETD5-KD DEGs
N.S.
decreased
increased
2nd degree target
1st degree target
adj. p = 2.6e-245
−log10 adj. p-value
log2 fold change
B
ASD Genes in NPC GRN
Consensus-ASD
HC-SFARI
Other
Regulator
Target
C
Central Genes
SysID
UV response DN
G2M checkpoint
somatic CNV
mitotic spindle
SFARI
HC-SFARI
syndromic
de novo SNV or indel
Consensus-ASD
−log10 adj. p-value
E
CHD8 Targets
CHD8 1˚ Regulon
HC-SFARI
CHD8 2˚ Regulon
Consensus-ASD
SFARI
SETD5 DEGs
SETD2 DEGs
SysID
KMT2E DEGs
adj. p−value
< 0.0001
< 0.001
Enrichment (Odds Ratio)
D
Top GRN Regulators Driving Convergence
GLYR1
HMGA2
RREB1
KDM3B
KDM1A
GTF2I
TRIM24
BAZ2A
LBR
PHF14
CHD2
KDM5A
BAZ1A
ZNF608
CBX5
ZNF462
KMT2A
CHD8
HIF1A
ADNP
ZNF532
ZEB2
KDM5B
POU2F1
BAZ1B
PBRM1
NFE2L2
YY1
TEAD1
CREBBP
PRDM2
TMF1
SMARCA5
GPBP1
EP300
MGA
SETD5
RFX7
ZMYND11
KMT2E
ZZZ3
CHD7
ATRX
BPTF
PURB
LCORL
ZFHX4
SETD2
ZNF655
ZNF148
PHF20L1
EEA1
ZNF292
PHF6
AHCTF1
BRWD1
ZNF326
KMT2C
JMJD1C
GLIS3
VEZF1
HIVEP1
ZNF518A
SPEN
CHD1
REST
ASH1L
POU3F2
PHF3
NSD1
ATAD2
TET1
ZNF91
SHPRH
ZNF644
ZNF770
ZNF609

Figure 3

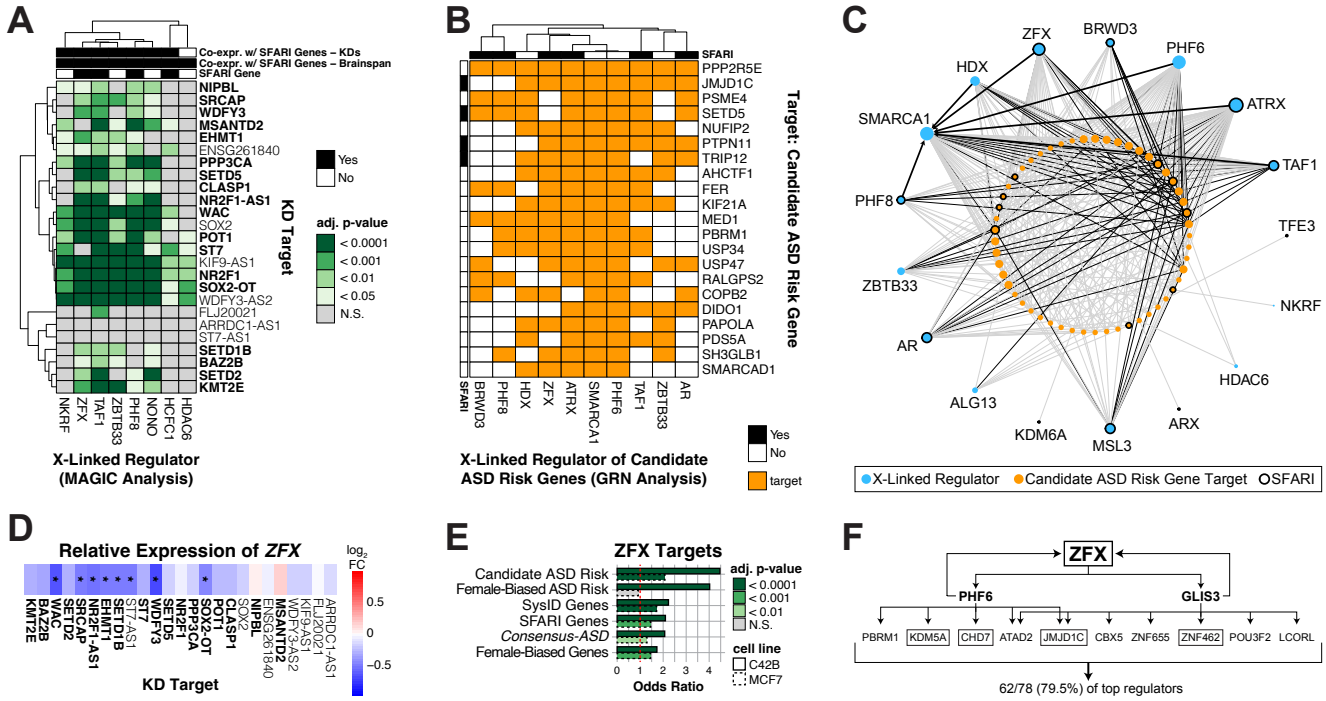
A
Co-expr. w/ SFARI Genes – KDs
Co-expr. w/ SFARI Genes – Brainspan
SFARI Gene
NIPBL
SRCAP
WDFY3
MSANTD2
EHMT1
ENSG261840
PPP3CA
SETD5
CLASP1
NR2F1-AS1
WAC
SOX2
POT1
ST7
KIF9-AS1
NR2F1
SOX2-OT
WDFY3-AS2
FLJ20021
ARRDC1-AS1
ST7-AS1
SETD1B
BAZ2B
SETD2
KMT2E
KD Target
Yes
No
adj. p-value
< 0.0001
< 0.001
< 0.01
< 0.05
N.S.
NKRF
ZFX
TAF1
ZBTB33
PHF8
NONO
HCFC1
HDAC6
X-Linked Regulator
(MAGIC Analysis)
B
SFARI
PPP2R5E
JMJD1C
PSME4
SETD5
NUFIP2
PTPN11
TRIP12
AHCTF1
FER
KIF21A
MED1
PBRM1
USP34
USP47
RALGPS2
COPB2
DIDO1
PAPOLA
PDS5A
SH3GLB1
SMARCAD1
Target: Candidate ASD Risk Gene
BRWD3
PHF8
HDX
ZFX
ATRX
SMARCA1
PHF6
TAF1
ZBTB33
AR
Yes
No
target
X-Linked Regulator of Candidate
ASD Risk Genes (GRN Analysis)
C
ZFX
BRWD3
PHF6
HDX
ATRX
SMARCA1
TAF1
PHF8
TFE3
ZBTB33
NKRF
AR
HDAC6
ALG13
ARX
KDM6A
MSL3
X-Linked Regulator
Candidate ASD Risk Gene Target
SFARI
D
Relative Expression of ZFX
log2 FC
0.5
0
−0.5
KMT2E
BAZ2B
WAC
SETD2
SRCAP
NR2F1-AS1
SETD1B
EHMT1
ST7-AS1
ST7
WDFY3
SETD5
NR2F1
PPP3CA
SOX2-OT
POT1
CLASP1
SOX2
NIPBL
ENSG261840
MSANTD2
WDFY3-AS2
KIF9-AS1
FLJ20021
ARRDC1-AS1
KD Target
E
ZFX Targets
Candidate ASD Risk
Female-Biased ASD Risk
SysID Genes
SFARI Genes
Consensus-ASD
Female-Biased Genes
0
1
2
3
4
Odds Ratio
adj. p-value
< 0.0001
< 0.001
< 0.01
N.S.
cell line
C42B
MCF7
F
ZFX
PHF6
GLIS3
PBRM1
KDM5A
CHD7
ATAD2
JMJD1C
CBX5
ZNF655
ZNF462
POU3F2
LCORL
62/78 (79.5%) of top regulators

Figure 4

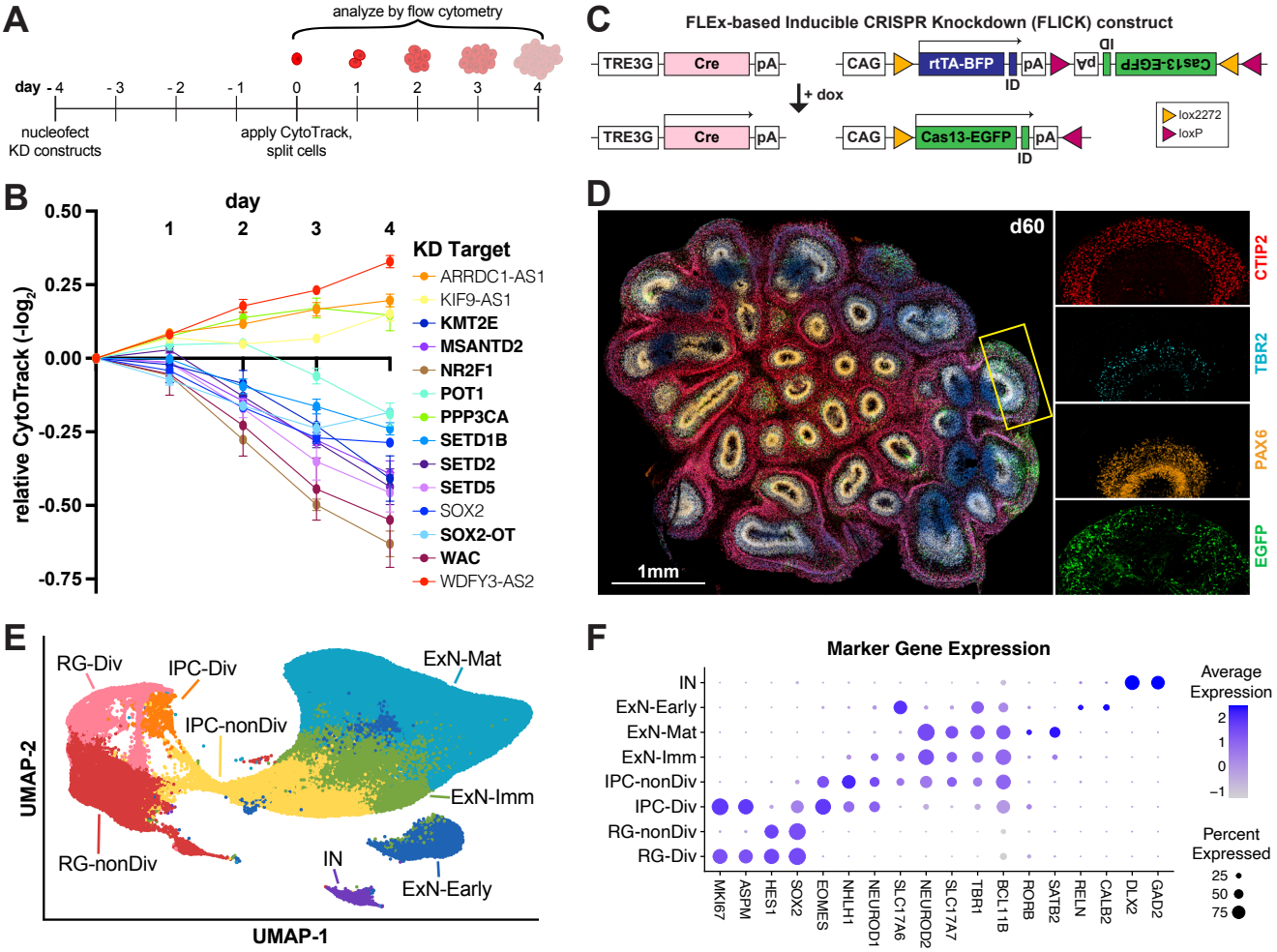
A
analyze by flow cytometry
day -4 -3 -2 -1 0 1 2 3 4
nucleofect KD constructs
apply CytoTrack, split cells
B
day
1 2 3 4
relative CytoTrack (-log2)
0.50
0.25
0.00
-0.25
-0.50
-0.75
KD Target
ARRDC1-AS1
KIF9-AS1
KMT2E
MSANTD2
NR2F1
POT1
PPP3CA
SETD1B
SETD2
SETD5
SOX2
SOX2-OT
WAC
WDFY3-AS2
C
FLEx-based Inducible CRISPR Knockdown (FLICK) construct
TRE3G
Cre
pA
+ dox
CAG
rtTA-BFP
ID
Cas13-EGFP
lox2272
loxP
D
d60
1mm
CTIP2
TBR2
PAX6
EGFP
E
RG-Div
IPC-Div
IPC-nonDiv
ExN-Mat
ExN-Imm
RG-nonDiv
IN
ExN-Early
UMAP-2
UMAP-1
F
Marker Gene Expression
IN
ExN-Early
ExN-Mat
ExN-Imm
IPC-nonDiv
IPC-Div
RG-nonDiv
RG-Div
MKI67
ASPM
HES1
SOX2
EOMES
NHLH1
NEUROD1
SLC17A6
NEUROD2
SLC17A7
TBR1
BCL11B
RORB
SATB2
RELN
CALB2
DLX2
GAD2
Average Expression
2
1
0
−1
Percent Expressed
25
50
75

Figure 5

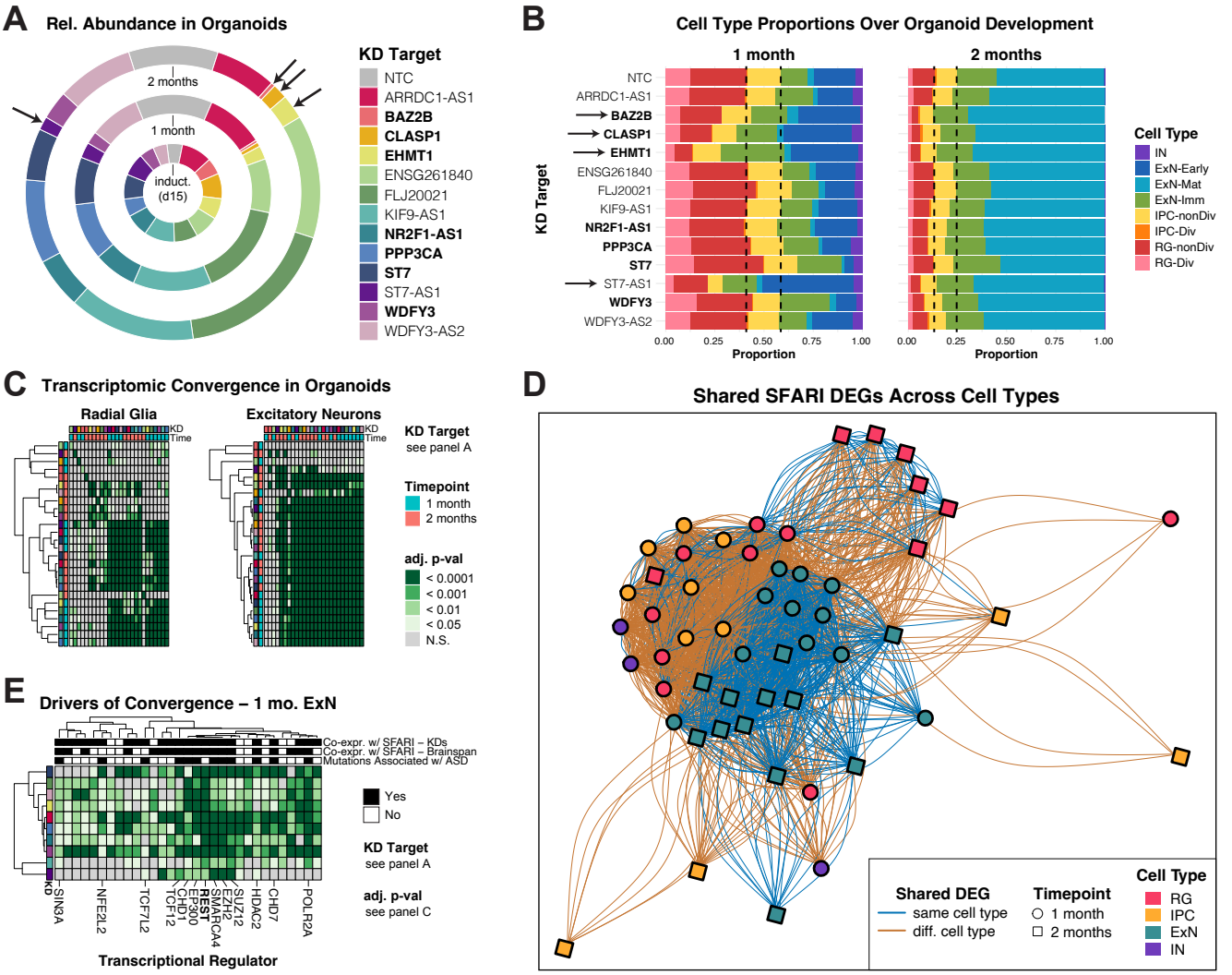
A
Rel. Abundance in Organoids
2 months
1 month
induct. (d15)
KD Target
NTC
ARRDC1-AS1
BAZ2B
CLASP1
EHMT1
ENSG261840
FLJ20021
KIF9-AS1
NR2F1-AS1
PPP3CA
ST7
ST7-AS1
WDFY3
WDFY3-AS2
B
Cell Type Proportions Over Organoid Development
1 month
2 months
KD Target
Proportion
Cell Type
IN
ExN-Early
ExN-Mat
ExN-Imm
IPC-nonDiv
IPC-Div
RG-nonDiv
RG-Div
C
Transcriptomic Convergence in Organoids
Radial Glia
Excitatory Neurons
KD
Time
KD Target
see panel A
Timepoint
1 month
2 months
adj. p-val
< 0.0001
< 0.001
< 0.01
< 0.05
N.S.
D
Shared SFARI DEGs Across Cell Types
Shared DEG
same cell type
diff. cell type
Timepoint
1 month
2 months
Cell Type
RG
IPC
ExN
IN
E
Drivers of Convergence – 1 mo. ExN
Co-expr. w/ SFARI – KDs
Co-expr. w/ SFARI – Brainspan
Mutations Associated w/ ASD
Yes
No
KD Target
see panel A
adj. p-val
see panel C
KD
SIN3A
NFE2L2
TCF7L2
TCF12
CHD1
EP300
REST
SMARCA4
EZH2
SUZ12
HDAC2
CHD7
POLR2A
Transcriptional Regulator

Figure 6

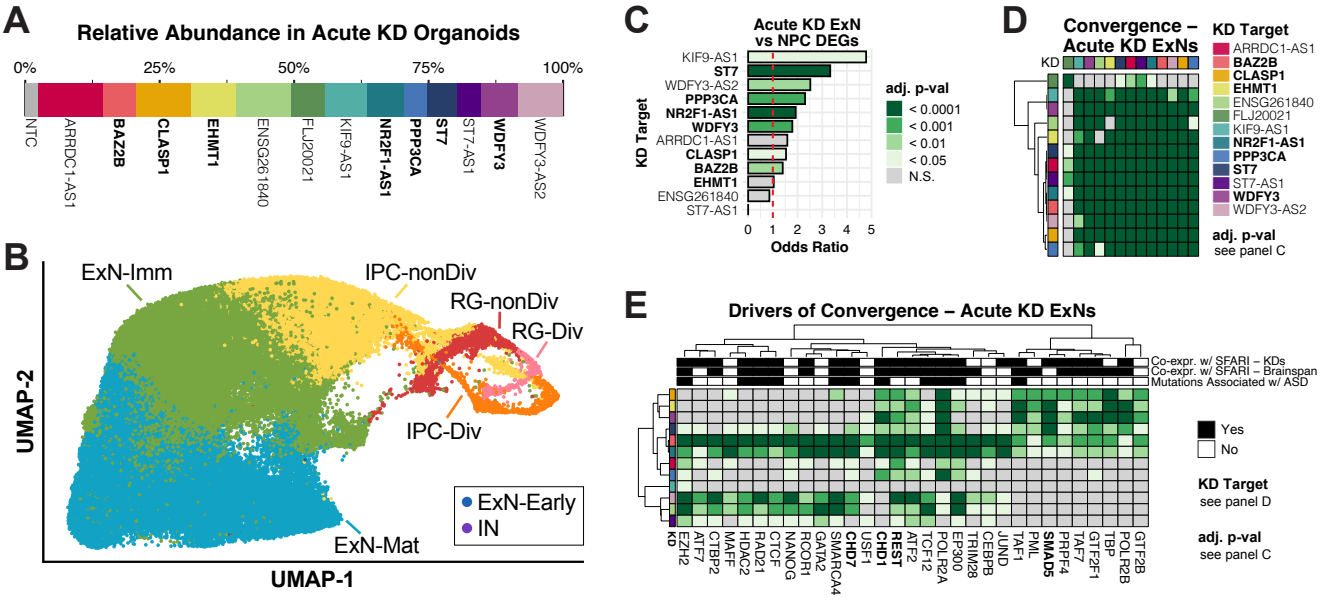
A
Relative Abundance in Acute KD Organoids
0%
25%
50%
75%
100%
NTC
ARRDC1-AS1
BAZ2B
CLASP1
EHMT1
ENSG261840
FLJ20021
KIF9-AS1
NR2F1-AS1
PPP3CA
ST7
ST7-AS1
WDFY3
WDFY3-AS2
B
ExN-Imm
IPC-nonDiv
RG-nonDiv
RG-Div
IPC-Div
ExN-Mat
ExN-Early
IN
UMAP-2
UMAP-1
C
Acute KD ExN vs NPC DEGs
KD Target
KIF9-AS1
ST7
WDFY3-AS2
PPP3CA
NR2F1-AS1
WDFY3
ARRDC1-AS1
CLASP1
BAZ2B
EHMT1
ENSG261840
ST7-AS1
0 1 2 3 4 5
Odds Ratio
adj. p-val
< 0.0001
< 0.001
< 0.01
< 0.05
N.S.
D
Convergence – Acute KD ExNs
KD
KD Target
ARRDC1-AS1
BAZ2B
CLASP1
EHMT1
ENSG261840
FLJ20021
KIF9-AS1
NR2F1-AS1
PPP3CA
ST7
ST7-AS1
WDFY3
WDFY3-AS2
adj. p-val
see panel C
E
Drivers of Convergence – Acute KD ExNs
Co-expr. w/ SFARI – KDs
Co-expr. w/ SFARI – Brainspan
Mutations Associated w/ ASD
Yes
No
KD Target
see panel D
adj. p-val
see panel C
KD
EZH2
ATF7
CTBP2
MAFF
HDAC2
RAD21
CTCF
NANOG
RCOR1
GATA2
SMARCA4
CHD7
USF1
CHD1
REST
ATF2
TCF12
POLR2A
EP300
TRIM28
CEBPB
JUND
TAF1
PML
SMAD5
PRPF4
TAF7
GTF2F1
TBP
POLR2B
GTF2B

Figure 7